Clocking Sleep: Role of dorsolateral clock neurons in the sleep circuit of *Drosophila melanogaster*

A Thesis

Submitted for the Degree of

Master of Science

By

SAHELI ROY

Neuroscience Unit

Jawaharlal Nehru Centre for Advanced Scientific Research

(A Deemed University)

Bangalore – 560 064, India

April 2019

Dedicated to the six-legged, red-eyed, tiny-brained creatures of wonder

Table of Contents

Declaration

I hereby declare that the thesis entitled '**Clocking Sleep: Role of dorsolateral clock neurons in the sleep circuit of *Drosophila melanogaster***' submitted towards the fulfillment of Master of Science degree is the result of investigations carried out by me during June 2018 to April 2019 under the supervision of Dr. Sheeba Vasu, at Behavioral Neurogenetics Laboratory, Neuroscience Unit, Jawaharlal Nehru Centre for Advanced Scientific Research, India. The work incorporated in this thesis have not been submitted by me for any other degree elsewhere.

In keeping with the practice of reporting scientific observations, due acknowledgement has been given when describing the work and findings of other investigators. Any omission that may have occurred due to misjudgment or oversight, is deeply regretted.

Saheli Roy

Place: Bangalore

Date: 5th May, 2019

Behavioral Neurogenetics Laboratory

NEUROSCIENCE UNIT

JAWAHARLAL NEHRU CENTRE FOR ADVANCED SCIENTIFIC RESEARCH

P.O. BOX - 6436, JAKKUR, BANGALORE - 560 064, INDIA

CERTIFICATE

This is to certify that the work described in this thesis entitled '**Clocking Sleep: Role of dorsolateral clock neurons in the sleep circuit of *Drosophila melanogaster***' is the result of studies carried out by Ms. Saheli Roy in the Behavioral Neurogenetics Laboratory of Jawaharlal Nehru Centre for Advanced Scientific Research, Jakkur, Bangalore 560 064, under my supervision, and that the results discussed in this thesis have not previously formed the basis for award of any other diploma, degree or fellowship.

Dr. Sheeba Vasu

Associate Professor
Neuroscience Unit
JNCASR
Bangalore, India

Acknowledgements

I would like to express my sincere gratitude to my thesis advisor, Dr. Sheeba Vasu. Over the course of my lab rotation and thesis work, she helped me mature as a researcher, and inculcate a spirit of scientific temper. I am grateful to her to allow me sufficient freedom to develop my own research questions, and for providing guidance in interpreting the results. Her insightful comments during our project-related discussions has greatly helped me to shape my work. I am also thankful to my other departmental faculties – Dr. G. R. Ramesh, Prof. Maneesha Inamdar, Prof. Kaustav Sanyal, Prof. Udaykumar Ranga, Prof. Hemalatha Balaram, Prof. Anuranjan Anand, Prof. Namita Surolia, Prof. Tapas K. Kundu, Dr. Ravi Manjithaya and Dr. James P. Chelliah for their lab and course-work in the Integrated MS-PhD program, which taught me to appreciate my subject from a new perspective.

I would also like to thank my present and past lab members Sheetal, Viveka, Aishwariya, Aishwarya, Rutvij, Ankit, Jaimin, Sushma, Abhilash, Anuj, Manishi, Arijit and Chitrang for providing support and motivation. The question addressed in my thesis was originally framed by Sheetal as part of her PhD project. I developed my interest in studying sleep after encountering her PhD work, and during my lab rotation at BNL, she taught me to conduct sleep assays in flies. Viveka, Aisha and Iyer had shared many sound, senior-ly advice over the course of the last year, primarily teaching me to worry less. Most of my understanding of statistics comes from Rutvij's detailed explanations, and the Kruskal Wallis test in R was done by Abhilash. Ankit was a huge help during the fly brain dissections. The younger batch consisting of Lara, Christine, Akshaya, Pragya and Ranjitha helped keeping the lab lively with their funny antics. Also, without the technical assistance of Muniraju and Rajanna at fly kitchen, and of Ms. Suma in the confocal facility, it would have been impossible to timely finish my experiments.

My classmates Rashi, Irine, Chhavi, Ankit, Shubham and Kuladeep made my stay in JNCASR a wonderful experience. Rashi made up most of my memories at NVSH, while Irine participated in the occasional Room 158 midnight banter. Chhavi shared my love of adventure, and Ankit became my partner in crime over these three years. Shubham and Kuladeep kept us sane with their witty

remarks and PJs over the dinner table. I am grateful to everyone else at JNC, students and staff alike, who enriched my first experience of hostel living. I would also take this opportunity to thank my teachers and friends from Kolkata for cheering me up everytime the task-at-hand seemed daunting, and my family for their constant love and encouragement.

Lastly, I thank JNCASR for funding my study during MS, and for providing ample facilities, both academic and non-academic. Particularly, the fast and effective medical facilities provided by Dhanvantri had been hugely beneficial for me, and critical for my stay.

Abstract

Sleep is a state of reduced awareness and responsiveness, conserved among metazoans. Across species, this behavior has been defined as a homeostatic episode of rest, restricted by the circadian clock to an appropriate time of day. Yet, despite its ubiquity, we know very little about this behavior, including details about its regulatory mechanism. Though the circadian pacemaker and the sleep homeostat have long been proposed to interact in order to control sleep (Borbely, 1982); experimentally such an interaction has not been clearly elucidated thus far. This question was previously approached in our lab by conducting a screen in flies wherein membrane electrical properties of different subsets of circadian clock cells were modulated and the subsequent change in sleep measured (Potdar S., *PhD Thesis*). This screen resulted in identification of a certain circadian clock cell cluster, Lateral Dorsal Neurons (LN_ds) as being a potential modulator. Transient neuronal activation of LN_ds led to sleep loss, followed by a subsequent post-activation sleep recovery. Therefore, this neuronal cluster was hypothesized to be the cellular location where both the clock and the homeostat were functionally overlapping. While further characterizing the role of this heterogenous group of cells in sleep regulation, using a similar method of transient neuronal hyper-activation, I found that LN_ds differentially regulate sleep. Activation of a smaller population of cells within this cluster encodes sleep loss irrespective of external light condition, whereas the remaining cells do so only in presence of light. Interestingly, the behavior observed during hyper-activation of the latter group of cells at night suggested their involvement in sleep promotion. Overall, these preliminary results led me to hypothesize that LN_ds show functional heterogeneity within the sleep circuitry of *Drosophila melanogaster*.

CHAPTER 1: INTRODUCTION

1.1 Behavioral correlates of sleep:

1.1.1 What is sleep? Sleep is a state of behavioral quiescence with reduced sensory responsiveness. From the simple cnidarian, jelly-fish to human beings, sleep has been found to be a conserved behavior in the metazoan world (Allada & Siegel, 2008). Across species, this behavior has been defined as homeostatically regulated episode of rest, usually restricted to a particular time of day. A homeostatic regulatory mechanism signifies that sleep loss, either in duration or intensity, is recovered via sleep rebound – a compensatory mechanism which allows enhancement of sleep quantity or quality, either before or during the next sleep episode. Other than the sleep homeostat, another physiological entity that determines sleep is the circadian clock (Latin, *circa* meaning approximately, *diem* meaning a day). The clock times this behavior in accordance to the ecological niche of the organism, such that predatory risks are minimized, and availability of food and potential mates maximized. Sleep is also easily reversible, albeit at a high stimulus intensity. This characteristic of increased arousal threshold differentiates sleep from behavioral rest (immobile wakefulness), while easy reversibility distinguishes it from anesthesia, coma and hibernation. Homeostatic control is another unique distinction, separating sleep from rest. Additionally, sleep is also associated with a species-specific posture, resting place and behavioral attributes like yawning and others (Campbell & Tobler, 1984).

Several decades of human sleep research in 1900s helped to understand how these two distinct processes, i.e. homeostatic and clock regulation, control sleep. In 1982, Alexander Borbély combined these two processes to generate a quantitative model of sleep/wake regulation (Borbély, 1982), which was later refined by Daan, Beersma and Borbély (Daan *et al.*, 1984). This 'two process model' (Figure 1.1) explained sleep need/propensity to consist of two components – a wake-independent sleep need controlled by the circadian clock (process C) that oscillates throughout the day in order to temporally restrict sleep; and a prior wake-dependent homeostatic process (process S) that increases as a function of time spent since the termination of the last sleep episode (Borbély, 1982). Later, further modifications to this model were proposed, the first of which was to introduce gating (Daan *et al*., 1984). The homeostatic process was modelled to have two thresholds, such that sleep is initiated upon reaching the lower threshold and terminated at the higher threshold. These thresholds were proposed to be under the control of the circadian clock

generated oscillations in sleep need. This, along with several newer additions to the model have been able to explain many of the empirical results discovered more recently in sleep research (Borbély *et al.*, 2016).

Other than these behavioral changes between wake and sleep, brain electrophysiological changes are also associated with the sleeping state. In 1924, Hans Berger first observed that brain waves differed between an awake and sleeping human. It is now known that these waves correspond to neuronal activity taking place in the brain, and stages in sleep can be distinguished on the ensuing rhythmic pattern. In general, birds and mammals exhibit two broad sleep stages – REM (Rapid Eye Movement) and non-REM. REM sleep is characterized by an active brain, but paralyzed skeletal muscles. Thus, during REM sleep the EEG recordings are characterized by small amplitude and high frequency, similar to the highly active, awake brain state. However, during non-REM sleep the brain shows reduced, synchronous electrical activity characterized by waves of high amplitude and low frequency (McCarley, 2007). Such slow wave activity also correlates with the strength of stimulus needed to awaken an individual (lower the frequency, higher the stimulus), hence is considered to be a measure of sleep depth. The homeostatically defined 'Process S' in Borbély's model was also based on measurement of this slow wave activity (Borbély, 1982).

Even though sleep research on humans is nearly a century old, still many details regarding this behavior remain unknown. We are yet to find answers to the questions of 'why we sleep?' and 'how sleep is regulated?' Therefore, to better understand this elusive behavior, it is important to unravel the genetic and neuronal circuitry controlling it. Hence, for the past several years simpler, genetically accessible model organisms are being used to study sleep including *Caenorhabditis elegans*, *Drosophila melanogaster* and *Danio rerio* (reviewed in Allada & Siegel, 2008). Even though the electrophysiological signatures of these simpler vertebrates and non-vertebrates markedly differ from mammalian recordings, yet these studies can be conducted based on the conserved behavioral correlates of sleep described previously.

1.1.2 *Drosophila* as a model organism for studying sleep – In 2000, two groups independently observed that in *Drosophila melanogaster*, inactivity/rest corresponded to all the behavioral

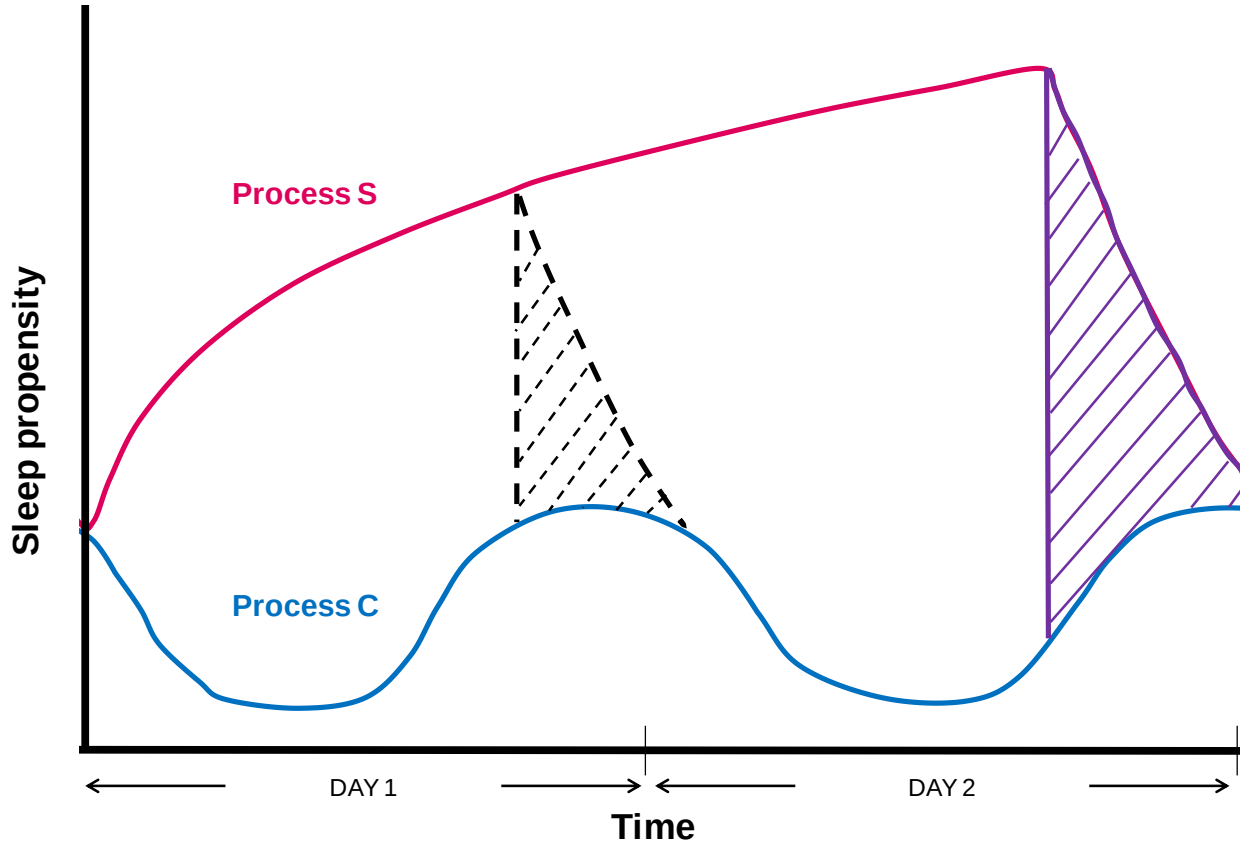

Figure 1.1. ***Two-process model of sleep regulation*****.** At a given time, sleep propensity is a function of two processes – sleep debt incurred by the sleep homeostat (Process S) and daily oscillation of circadian clock-controlled sleep need (Process C). Sleep propensity determined by the sleep homeostat is lowest at the end of a sleep episode, increases with the amount of time spent awake and when it crosses an upper threshold, the next sleep episode begins. In contrast, the clock-controlled sleep propensity is not dependent on prior wake time, and cycles throughout the day. According to this model, an interaction of these two processes bring about sleep when the difference between them are minimum. Normally, sleep would begin at the black, dashed vertical line, and over the course of a sleep episode (black hatched lines), sleep need would come back to baseline (black, dashed curve) from which it would again begin to rise post sleep termination. In the figure however, the sleep pressure does not get released because forced sleep deprivation takes place during the organism's usual sleep time on day 1. Hence, the Process S continues to rise until the circadian clock favors sleep onset on the next day (purple vertical line). The sleep rebound post-deprivation (purple hatched lines) is discharged from a higher value, hence it results in an increase in sleep duration, or intensity, or both. Based on the study by Borbély, 1982.

features of sleep (Hendricks *et al*., 2000 and Shaw *et al*., 2000). Sleep in *Drosophila* showed (i) consolidated circadian bouts of immobility, (ii) a species-specific posture and/or resting place, (iii) an increased arousal threshold, and (iv) a homeostatic regulatory mechanism (Hendricks *et al*., 2000), thus fulfilling all the criteria used to define sleep (Campbell & Tobler, 1984). It was also found that flies respond to sleep-inducing (example, anti-histamines) and sleep-inhibiting (example, caffeine) agents just like mammals, highlighting the conserved neural mechanisms in both these organisms (Hendricks *et al*., 2000 and Shaw *et al*., 2000). In a similar vein, young flies slept more, and it took them three days post-eclosion to reach the adult pattern of sleep (Shaw *et al*., 2000). Older flies (> 30 days) even showed sleep fragmentation and decreased arousal threshold, similar to mammals (Koh *et al*., 2006 and Vienne *et al*., 2016). Moreover, flies also displayed changes in brain activity (detected by quantifying local field potential) during awake and sleeping states, with low brain activity correlating with sleep (Nitz *et al*., 2002). Even within a single sleep episode changes could be detected in local field potential (LFP), denoting the existence of deeper and lighter sleep stages, not unlike mammals (van Alphen *et al*, 2013). Altogether, these findings established *D. melanogaster* as a potent model organism for studying sleep.

Sleep profile for wild-type flies is bimodal, with a midday siesta, and longer, consolidated bouts of sleep at night. In a day, it is only during the morning (dawn) and evening (dusk) bouts of activity that their sleep is either minimal or completely absent. In order to distinguish between sleep and inactivity, it was determined that an inactivity bout of five or more minutes would be considered sleep. This cut-off was decided on the basis of flies responding to stimuli – behaviorally awake flies readily responded to these stimuli, while flies quiescent for five minutes or longer generally failed to do so (Hendricks *et al*., 2000 and Shaw *et al*., 2000). Fly sleep architecture was found to be sexually dimorphic (unlike humans), with males showing greater daytime siesta (Huber *et al*., 2004). Therefore, female flies were used in this study because their daytime sleep is statistically lower compared to nighttime sleep. Additionally, fly sleep is highly variable even in a genetically homogenous population, and can easily sustain changes caused by slight environmental variations. Hence, a standard practice was followed in this study wherein parental fly lines were backcrossed to *Iso*31 or w^{1118} background so as to genetically homogenize all flies prior to conducting sleep assays.

Drosophila being the ideal model system to conduct studies of behavioral genetics, several cellular and molecular players regulating sleep could be identified in flies heretofore unknown in mammals. Much of what we know about sleep regulation today has been a contribution of *Drosophila* biology. Genes and circuits identified in flies have bettered our understanding of how sleep is controlled – including the two-process model of sleep regulation. Thus, this system can be utilized to answer one of the most relevant question in the field – how the circadian clock and sleep homeostat interact to bring about sleep? Even though I will not be mentioning the details of fly genes regulating sleep (reviewed in Cirelli, 2009), I will briefly review the identified neuronal circuit modulating sleep before moving on to discuss my study on the interaction of circadian clock and sleep homeostat.

1.2 Neuronal correlates of sleep in *Drosophila*:

1.2.1 Homeostatic circuitry – By definition, a homeostat needs to perform four functions – sense the current measure of a variable in a system, compare it to a predefined threshold, compute the necessary action to be taken depending on the deviation of the variable from the threshold, and activate the system to perform this action. In *Drosophila*, the four major neuropil structures known to be involved in sleep are Mushroom Body (MB), Pars Intercerebralis (PI), Fan-shaped Body (FB) and Ellipsoid Body (EB) (Figure 1.2 A). All of these structures also mediate several other functions including but not restricted to, olfactory learning and memory (Heisenberg *et al*., 1985) and locomotion (Martin *et al*., 1998) in MB, circadian control of locomotion (Cavanaugh *et al*., 2014) in PI, and visual pattern memory in FB and EB (Pan *et al*., 2009). Therefore, they form part of the higher center in fly brain and are relevant sites for hosting sleep homeostatic circuitry.

One of the first anatomical locus identified to control sleep in flies was the Mushroom Body (Joiner *et al.*, 2006 and Pitman *et al*., 2006). Both the groups identified MB as a sleep-controlling center using two different screening strategies, and observed MBs to perform both sleep-inducing and inhibiting functions. The neuronal circuit underlying these effects were later resolved upon identification of two segregated microcircuits within the MB (Sitaraman *et al*., 2015). Kenyon cells (KCs), based on their axonal innervation pattern within different lobes of mushroom bodies, can form two distinct classes – sleep-promoting and wake-promoting. This sleep regulatory

information is communicated to two functionally distinct MBONs (Mushroom Body Output Neurons) via excitatory synaptic microcircuits, such that sleep-inducing KCs increase sleep by preferentially activating sleep-promoting MBONs, and sleep-inhibiting KCs decrease sleep by preferentially activating wake-promoting MBONs. Moreover, it was shown that these microcircuits encode for physiological sleep need: electrical activity of the sleep-inducing circuit increases post exogenous sleep deprivation, while activity in one sleep-inhibiting circuit decreases and the other remains unchanged. To summarize, mushroom bodies have a complex, multi-faceted role to play in sleep regulation (Artiushin & Sehgal, 2017).

The next brain region to be implicated in sleep was Pars Intercerebralis (Foltenyi *et al.*, 2007). The effect of EGFR on sleep induction was localized to the PI, even though a later study established arousal-promoting effect of the PI to a different subset of neurons (Crocker *et al.*, 2010). Octopamine was found to be an arousal-mediating neurotransmitter in flies (Crocker & Sehgal, 2008). These octopaminergic neurons connected post-synaptically with the PI, and external octopamine administration increased electrical activity of the sleep-inhibiting neuronal subset (Crocker *et al.*, 2010). Similar to MB, both sleep-inducing and inhibiting functions have thus been mapped to the PI, even though no homeostatic function has yet been located. However, the PI was also found to serve as an output pathway for circadian information (Jaramillo *et al*., 2004), and had been hypothesized to function as an integrator of homeostatic and circadian signals (Crocker *et al.*, 2010).

Fan-shaped Body (FB), a part of the Central Complex (CC) structure, was identified in another screen targeted to isolate sleep-inducing brain regions (Donlea *et al*., 2011). It was found that *Exfl2* cells projecting into the dorsal fan-shaped body promote sleep when activated. Moreover, these cells changed their membrane excitability in response to a change in sleep drive, meaning their excitability increased after sleep loss, and returned to baseline post-recovery (Donlea *et al.*, 2014). This physiological switching between ON and OFF states are mediated by regulating two types of potassium channel conductance (Pimentel *et al*., 2016). During sleep induction, high excitability of dFB neurons are maintained by activation of *Shaker* and *Shab* channels allowing fast repolarization. Also, potassium leak channel *Sandman* is internalized during this state, which however recycles back to the plasma membrane in response to wake-promoting dopaminergic

signal to silence the dFB neurons. The modulation of sleep by dFB neurons fundamentally correlates with the theoretically defined Process S in Borbély's two-process model and possibly function as the output arm of the sleep homeostat.

The sleep drive, however, is generated by another neuropil in the central complex called Ellipsoid Body (Liu *et al*., 2016). The R2 ring neurons within the ellipsoid body encode for higher sleep pressure by increasing its neuronal activity and strengthening its pre-synaptic connections. Once the sleep drive dissipates either during night-to-day transition or after completion of a rebound sleep episode, the neuronal activity returns back to baseline. Appropriately, the R2 ring neurons function upstream of the dorsal fan-shaped body, and in turn activate the dFB neurons. On the other hand, excitation of the dFB neurons inhibit certain interneurons of the central complex (termed 'helicon cells'), which synapse onto the R2 neurons of EB (Donlea *et al*., 2018). This recurrent neuronal circuitry ensures that activation of the effector (dFB) by the integrator (EB) initiates release of the accumulated sleep pressure, which in turn suppresses EB excitation via the helicon cells to revert the integrator back to baseline conditions.

1.2.2 Circadian circuitry – Though the homeostat determines the quantity and quality of sleep required at a given time, the circadian clock regulates the timing of an organism's activity-sleep bouts. In *Drosophila*, the circadian clock is well elucidated both at the molecular and cellular levels, unlike the sleep circuit. Here, I first review details of the molecular clock before moving on to the cellular circuit.

In brief, the *Drosophila* molecular clock consists of two interlocked transcriptional-translational feedback loops (reviewed extensively in Hardin, 2005; Rosato *et al*., 2006 and Zheng & Sehgal, 2008). The central players for both these loops are two transcriptional factors – *Clock* and *Cycle*. CLK/CYC bind to E-box regulatory sequences of both *Period* (*Per*) and *Timeless* (*Tim*) genes, allowing their transcription to occur between midday to early evening. Thereafter, their mRNAs peak followed by a peak in their protein levels around late night. Once both the proteins accumulate in the cytosol, they form a stable complex that can cross the nuclear membrane to inhibit their own transcription. Consequently, their mRNA levels start to decline, followed soon after by a drop in protein quantity. During the same time of *Per*/*Tim* transcription, CLK/CYC also bind to E-boxes

of *Vrille* (*Vri*) and *Par domain protein 1ε* (*Pdp1ε*) to initiate their transcription. VRI protein accumulates in phase with its mRNA and inhibits transcription of *Clk* by binding to V/P box sequence during early night. PDP1ε starts accumulating from midnight and restores *Clk* transcription. Though this molecular oscillation is sufficient to self-sustain the clock under constant conditions, it also needs to correctly phase itself according to the cycling environmental factors, the strongest of them being light. Most crucial in this pathway is the blue light photoreceptor CRYPTOCHROME (CRY), that can change its structural conformation upon stimulation by light, allowing it to bind to TIM and trigger its degradation. Depending on the time of the day (phase of the clock), TIM degradation can differently affect PER nuclear localization, either delaying or advancing it, hence phase shifting the clock.

Components of this molecular clock are found in approximately 150 neurons in the fly brain, which form the circadian pacemaker circuit (reviewed in Sheeba, 2008 and Nitabach & Taghert, 2008). These neurons are bilaterally distributed and can be broadly divided into two clusters based on their anatomical location – dorsal neurons (DNs) and lateral neurons (LNs) (Figure 1.2 B). As the name suggests, the dorsal neurons are located in the dorsal protocerebrum, and consist of three subgroups – ~16 DN_1, a pair of DN_2 and ~40 DN_3 neurons in each brain hemisphere. These dorsal neurons are usually associated with integrating environmental inputs and accordingly adjust the clock. They are implicated in temperature entrainment and can maintain molecular oscillations under constant light. In contrast, the lateral neurons can be divided into 6 dorsal lateral neurons (LN_ds) and 9 ventral lateral neurons (LN_vs). The latter group is further subdivided based on cellular size – 4 large ventral lateral neurons (l-LN_v) and 4 small ventral lateral neurons (s-LN_v), both subsets being PDF^{+ve}, and a PDF^{-ve} 5^{th} s-LN_v. Most of these cells are CRY^{+ve} (except for 3 LN_ds), hence molecularly arrhythmic under constant illumination. The four PDF^{+ve} sLN_vs are the primary contributors in maintenance of behavioral rhythmicity under constant darkness. Under cycling light-dark conditions however, both LN_vs (morning neurons) and LN_ds (evening neurons) are essential to maintain a bimodal activity profile, characteristic of wild type flies. Pigment Dispersing Factor (PDF) is the best characterized neurotransmitter in this circuit and is required to maintain behavioral rhythmicity in constant darkness. It is released in a circadian fashion and functions in synchronizing the circadian network, including the very cells it is released from. However, absence of PDF does not result in complete abolition of behavioral rhythmicity, thus

suggesting the role of other circadian molecules (reviewed in Beckwith & Ceriani, 2015). Other than PDF, neuropeptides identified in the *Drosophila* clock cluster include Neuropeptide F (NPF), Small Neuropeptide F (sNPF) and Ion Transport Peptide (ITP). All of these have been proposed to work as intra-network communication signals, with sNPF being expressed among sLN_v and 2 LN_ds (both CRY^{+ve}), NPF in few lLN_vs, 5^{th} sLN_v and 3 LN_ds (2 CRY^{+ve} and 1 CRY^{-ve}) and ITP in 5^{th} sLN_v and 1 LN_d (CRY^{+ve}/$sNPF^{-ve}$). Apart from these neuropeptides, classical neurotransmitters such as acetylcholine, glutamate and GABA are also employed by this system. In summary, the network properties of the circadian circuit suggest its function as a multi-oscillator model, which needs to be strongly coupled in order to generate robust behavioral rhythms under changing environmental conditions.

1.2.3 Interaction of homeostatic and circadian circuitry – Having reviewed both the homeostatic and clock circuits, here I discuss the points of their interaction identified thus far. The empirical evidence that both these entities interact rather than act independently to determine sleep duration and intensity was first observed long back in humans (Akerstedt & Gillberg, 1981). However, the cellular correlates of this interaction haven't yet been clearly explicated in any organism. Only in recent years have a few studies identified *Drosophila* circadian neurons affecting sleep, detailed below.

The lateral ventral neuronal cluster has so far been most studied among all circadian neurons for its effect on sleep. They have been characterized as arousal-promoting neurons because increasing their neuronal activity using widely different methods have all resulted in decreasing sleep, especially at night (Sheeba *et al*., 2008; Parisky *et al.*, 2008 and Shang *et al.*, 2008). This sleep inhibitory effect of LN_vs is mediated via PDF, as flies lacking PDF signaling sleep more than controls (Sheeba *et al*., 2008 and Chung *et al.*, 2009). Among the LN_vs, activation of only the l-LN_vs is sufficient to hyper-activate flies at night (Sheeba *et al*., 2008 and Shang *et al.*, 2008). It has been identified that light activates l-LN_vs to promote arousal during day (Shang *et al.*, 2008), while GABAergic signals inhibit l-LN_vs to induce sleep at night (Parisky *et al.*, 2008; Chung *et al.*, 2009 and Liu *et al*., 2014). A recent study from our lab further elucidated the role of this arousal circuit by uncovering the downstream pathway from l-LN_vs. According to Potdar & Sheeba 2018, l-LN_vs receive activating signals during the day, which is communicated to s-LN_vs. In turn, s-LN_vs

inhibit dopaminergic neurons via PDF to promote wakefulness. At night, inhibition of l-LN_vs by GABA suppresses downstream inhibition of s-LN_vs, thus promoting sleep. In contrast, another study reported nighttime sleep-inducing function of s-LN_vs, wherein sNPF released by s-LN_vs acts on the wake-promoting l-LN_vs. Additionally, sNPF signalling was found to affect rebound sleep, thus suggesting its involvement with the sleep homeostat (Shang *et al*., 2013). No detailed study discussing role of LN_ds in sleep-wake regulation has yet been reported.

Several recent studies have established role of dorsal neurons in controlling sleep with respect to environmental inputs. Among the DNs, a subset of 5-6 DN_1s were first identified to suppress sleep during late night (in anticipation of dawn) via release of a neuropeptide DH31 in response to PDF signaling (Kunst *et al*., 2014). However, another group described DN_1s to promote sleep, especially during midday siesta, by inhibiting activity-promoting lateral neurons (both M and E cells) using glutamate (Guo *et al*., 2016). This suggests that the DN_1s function in the complex role of both sleep and wake promotion, the anatomical substrates for which have now been identified. The wake-promoting DN_1s (CRY^{-ve}) send projections to the PI (Barber *et al*., 2016 and Guo *et al*., 2018) communicating by temporal codes wherein during daytime DN_1s fire in irregular patterns that activate persistent firing of the arousal-promoting Dilp2+ neurons in the PI (Tabuchi *et al*., 2018). In contrast, the output of sleep-promoting DN_1s (CRY^{+ve}/$PDFR^{+ve}$) indirectly activate EB ring neurons, decreasing arousal and enhancing sleep (Guo *et al*., 2018). Another independent group identified the same pathway from DN_1 to EB via tubercular-bulbar (TuBu) neurons located in the anterior optic tubercle neuropil, however they described these DN_1s to inhibit the sleep-promoting TuBu neurons (Lamaze *et al*., 2018). Additionally, the DN_1p subset of neurons were also found to change their electrical activity upon receiving thermosensory inputs from peripheral organs. These neurons are excited upon cooling, and inhibited by heat, and under naturalistic temperature cycles phases sleep onset with cold temperature (Yadlapalli *et al*., 2018).

Even though all these studies attempted to study the interaction of the circadian clock and sleep homeostat, a direct evidence establishing interdependence of the clock and homeostat in regulating timing and quality of sleep has been limited. In an effort to do so, I examined the possible role of circadian pacemaker cells in regulating sleep homeostasis.

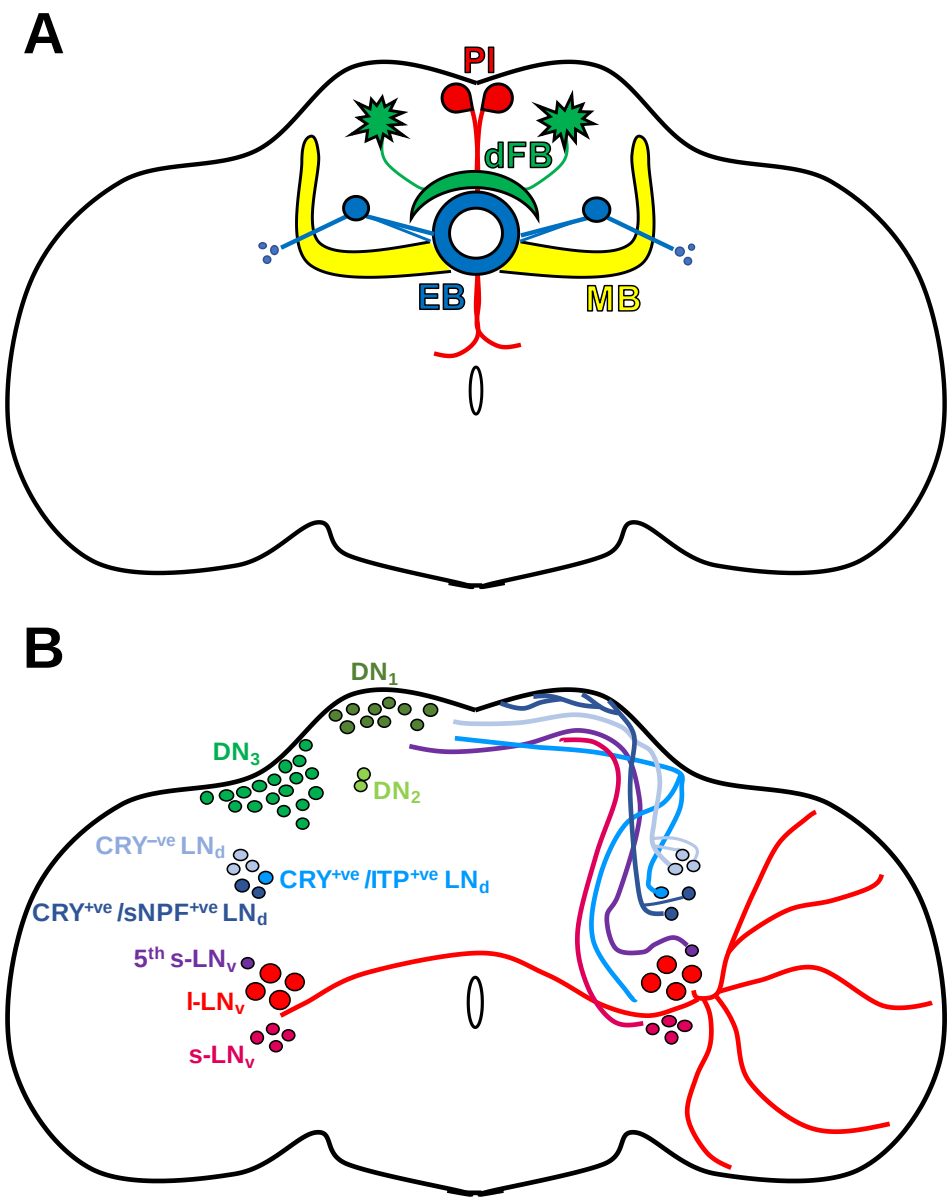

Figure 1.2. ***Diagrammatic representation of sleep homeostat circuit (A) and circadian pacemaker circuit (B) of Drosophila melanogaster.*** (A) The identified fly sleep homeostatic circuit consists of Mushroom Body (MB in yellow) – functional in both arousal and sleep promotion; Pars Intercerebralis (PI in red) – reported for both sleep and wake induction; R2 ring neurons and Ellipsoid Body (EB and adjacent cells, in blue) – considered as the integrator of sleep homeostat; and *Exfl2* cells and dorsal Fan-shaped Body (dFB and neighboring cells, in blue) proposed to be the output arm of the homeostat. (B) Circadian clock neurons located to the fly brain (left brain hemisphere) based on presence of functional molecular clock, and reported projection pattern of lateral neurons (right brain hemisphere; dorsal neurons not depicted for the sake of clarity). DN – dorsal neuron, divided into DN1, DN2 and DN3 based on anatomical location. LN – lateral neuron, LN_d – dorsal lateral neuron, LN_v – ventral lateral neuron. s-LN_v – small LN_v (PDF^{+ve}), 5^{th} s-LN_v – 5^{th} small LN_v (PDF^{-ve}), l-LN_v – large LN_v (PDF^{+ve}). All CRY^{+ve} LN_ds are also $PDFR^{+ve}$ (PDF Receptor). Projection of lateral neurons are shown as described by Schuber*t et al*., 2018.

CHAPTER 2: Function of LN_ds in sleep homeostatic circuit

2.1 Introduction:

In my previous chapter, I have elucidated details of the circadian clock and sleep homeostatic circuitry in *Drosophila melanogaster*. In flies, unlike the clock circuit, the sleep circuit has been studied less, and is yet to be mapped out in its functional entirety. However, it is now known that fly sleep results from an interaction between the circadian clock and sleep homeostat (reviewed in Chapter 1). To better understand modulation of sleep by the circadian clock, an approach previously taken in our lab was to test for sleep homeostasis mediated by circadian clock neurons (Potdar S., *PhD Thesis*). The method adopted was to electrically modulate membrane properties of different subsets of clock neurons in order to transiently activate them and study the subsequent effect on sleep (Table 2.1). This screen identified that only when a subset of lateral neurons, targeted by the driver *Dvpdf GAL4* (expressed in large and small ventral lateral neurons – PDF^{+ve} l- and s-LN_vs, PDF^{-ve} 5^{th} small ventral lateral neuron – 5^{th} s-LN_v, and lateral dorsal neurons - LN_ds) were hyper-excited by expressing the heat-activated *Drosophila* Transient Receptor Potential A1 *(dTRPA1)* channel (Hamada *et al*., 2008), a reduction in total sleep duration could be seen (compared to both the *GAL4* and *UAS* parental controls) (Figure 2.1 A). This sleep deprivation resulting from hyper-activation of *Dvpdf GAL4*-targeted neurons was found to be recovered post-activation, when compared to sleep during activation (Figure 2.1 B). A later assay also showed that this sleep recovery is significant when compared to pre-activation sleep duration (Potdar S. – personal communication). However, when lateral neurons targeted by another driver, *Pdf GAL4* (expressed only in PDF^{+ve} l- and s-LN_vs) were hyperexcited, it did not result in a similar sleep loss (Table 2.1 & Figure 2.1 A). A decrease was observed only in nighttime sleep but not during day, hence the total sleep duration remained significantly unaffected (Potdar S., *PhD Thesis*). Though the LN_vs have been previously reported to mediate arousal throughout the day, their hyper-excitation led to a reduction in nighttime sleep specifically (Parisky *et al*., 2008; Shang *et al*., 2008; Sheeba *et al*., 2008). Hence, it was proposed that the additional cells targeted by *Dvpdf GAL4*, namely 5^{th} sLN_v and LN_ds, might be coding for a state of sleep deprivation when hyper-activated, which is recovered post-activation with the activity levels getting restored. As this phenomenon of sleep rebound (gain in sleep post-sleep deprivation) is solely a function of the sleep homeostat, it was inferred that these additional cells, which are known to modulate evening peak of activity

under standard LD 12:12 cycles (Grima et al., 2004; Rieger et al., 2006; Stoleru et al., 2004), might also possess sleep homeostatic functions.

Upon finding the involvement of 'evening neurons' in sleep homeostasis, the next question asked was whether these cells required the intracellular molecular circadian clock to perform the homeostatic function (Potdar S., *PhD Thesis*). The basis of this question was rooted in the discovery that a functional molecular clock was required to maintain certain sleep homeostatic features – disruption of the clock (in whole-body mutants of *per*, *tim*, *clk* and *cyc*) abolished time-of-day dependent sleep recovery (Potdar S., *PhD Thesis*). However, when dominant negative forms of CLK and CYC were expressed using the *Dvpdf GAL4* driver, their sleep profiles did not vary from the controls. Moreover, the time-of-day dependent sleep homeostasis observed for control flies, but not in clock-mutants, was preserved in these flies with a dysfunctional molecular clock within the evening neurons. This suggested that a ticking circadian clock was not essential for these neurons to function as a sleep homeostat; indicating that they are located at the intersection of the circadian clock and the sleep homeostat with distinct independent functions in both processes (Potdar S., *PhD Thesis*).

Based on these results, I wished to further characterize the role of evening neurons in sleep. To do so, I employed two methods – I analyzed sleep patterns resulting from hyper-excitation of all subsets of lateral neurons in further details to better understand the underlying circuit, besides specifically targeting a subset of the evening neurons within the lateral neuronal cluster. However, as these two methods required me to use two different driver lines (*Dvpdf GAL4* and *Mai179 GAL4; Pdf GAL80*, respectively), the targeted LN_ds were mostly non-overlapping. Out of the seven pairs of evening neurons described, *Dvpdf GAL4* (Bahn *et al*., 2009) was reported to target 5^{th} s-LN_v, three CRY^{-ve} LN_ds and the CRY/ITP co-expressing LN_d (Schubert *et al*., 2018); while *Mai179 GAL4* (Siegmund & Korge, 2001) was reported to target 5^{th} s-LNv along with three CRY^{+ve} LNds (Rieger *et al*., 2009; Yoshii *et al*., 2008). Hyper-excitation under standard light-dark regime (henceforth referred to as high light intensity) in both these cases led to very distinct sleep phenotypes – the former resulted in total sleep loss as discussed, while in latter the effect was restricted to daytime sleep loss, only. Furthermore, with sleep loss being restricted only to daytime, and nighttime sleep being as high as during pre-activation, the sleep profile of *Mai179 GAL4; Pdf*

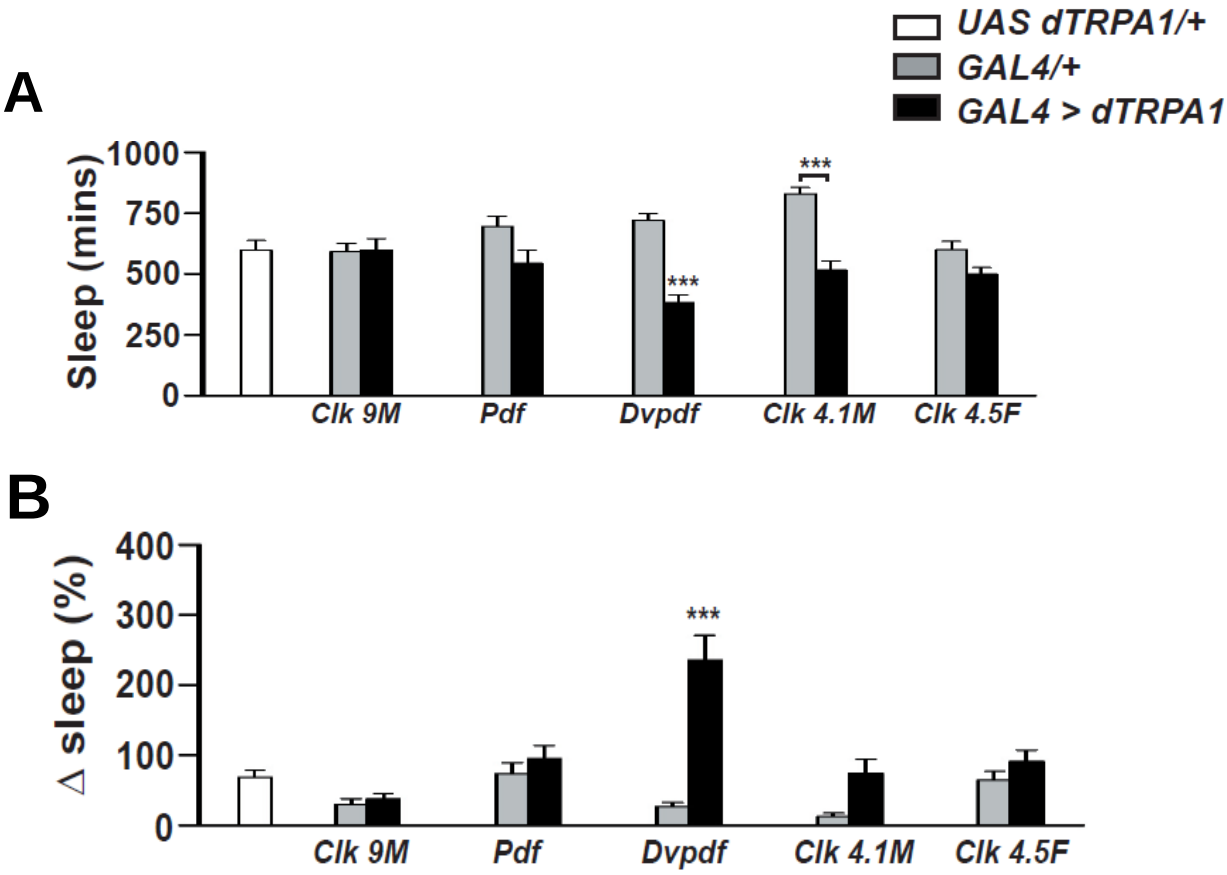

Table 2.1

Expressed in	s-LN_v	l-LN_v	LN_d	DN_1	DN_2	DN_3
Clk 9M GAL4	✓				✓	
Pdf GAL4	✓	✓				
Dvpdf GAL4	✓	✓	✓			
Clk 4.1M GAL4				✓		
Clk 4.5 F GAL4				✓		

Figure 2.1. ***Among all circadian clock neuronal subsets, only lateral neurons significantly affect sleep.*** (A) Averaged total sleep duration during hyper-excitation of clock neurons for two days at 29 °C. Sleep duration is significantly reduced relative to both parental controls only when all subsets of lateral neurons are targeted, as seen for *Dvpdf GAL4 > UAS dTRPA1* (Table 2.1). (B) Significant sleep recovery was seen in flies targeted using *Dvpdf GAL4* post-activation at 21 °C, when compared to sleep duration during activation. n = 23-32 flies. Error bars denote SEM. *p<0.05, **p<0.005, ***p<0.0005. Figures (A) and (B) are taken from Potdar S., *PhD Thesis*, JNCASR with permission.

GAL80 targeted flies showed a steep change during day-to-night transition. I hypothesized this abrupt change to be an interaction between light and electrical activity of the CRY^{+ve} LN_ds. To test this hypothesis, I carried out the same assay under dim light-dark regime (henceforth referred as low light intensity). The change in light intensity did not affect sleep when all subsets of lateral neuronal cluster was targeted, but changed the sleep pattern upon hyper-activation of few evening neurons. This suggested that among the LN_ds, there might be differential regulation of sleep.

2.2 Materials & Methods:

2.2.1 Fly Strains – Except for *Mai179 GAL4; Pdf GAL80*, all other fly strains that were used have been listed in Appendix 1, along with their source information. The fly line *Mai179 GAL4; Pdf GAL80* was created by me, for the purpose of restricting driver expression specifically to the evening neurons (Figure 2.2 C). All fly lines used in the assays described henceforth had previously been backcrossed to the standard *Iso*31 or w^{1118} background for at least five generations (around 2-3 years earlier). While conducting the assays, I further backcrossed *UAS dTRPA1* flies for two generations. All these fly lines were maintained on standard cornmeal medium under standard 12:12 hour light-dark cycles (LD 12:12) at 21 °C. Prior to the assay setup, the assayed flies were also briefly maintained under similar regime.

2.2.2 Immunocytochemistry – To visualize the neurons targeted by these driver lines, adult brain dissection was done in ice-cold PBS (Phosphate Buffered Saline). Thereafter, the brains were fixed using 4% paraformaldehyde (200-250 µl per well) for 30 mins at RT, on a shaker, followed by three washes of 10 mins duration each, in 0.5% PBT (0.5% TritonX100 in 1X PBS), also at RT. Blocking was done overnight (16 h) at 4 °C to reduce non-specific antibody binding using blocking solution (10% horse serum added to 0.5% PBT). The brains were then incubated in a primary antibody cocktail mix for 24 h, at 4 °C. The primary antibody solution was made using anti-GFP (1:3000, raised in chicken, Invitrogen #A10262) and anti-PDF (1:15000, raised in rabbit, M. Nitabach and donated by T.C. Holmes), prepared in blocking solution. After the primary incubation, six 0.5% PBT washes were given for 10 mins each at RT, followed by incubation with secondary antibody mix for 24 h, at 4 °C. The secondary antibody mix consisted of anti-chicken

Alexa Fluor 488 (1:3000, Invitrogen #A11039) and anti-rabbit Alexa Fluor 546 (1:3000, Invitrogen #A11035), also prepared in blocking solution. The secondary incubation was followed by six 0.5% PBT washes, 10 mins each, after which the brains were cleaned of extraneous tissue, and mounted on glass slides using 3:7 PBS:glycerol medium. Confocal images were taken on Zeiss LSM 880 microscope (with Airyscan, ZEISS, Oberkochen, Germany) with 40X (oil immersion) objective.

2.2.3 Sleep assays – Sleep was measured for 4-6 days old mated females, usually sexed one day prior to assay setup. During the assay, individual flies were housed within glass tubes (3 mm inner diameter, 5 mm outer diameter and 65 mm in length), containing sucrose food medium (5% sucrose and 2% agar) (Potdar & Sheeba, 2018) on one end, and a cotton plug on the other end. Mated females are regularly used for studying sleep, because they show marked differences between daytime and nighttime sleep duration. Sucrose-agar food is a standard preparation used for assaying mated females in order to prevent their eggs from hatching. This precaution is taken because presence of larvae within such confined quarters can disturb the usual fly activity pattern. The separation of females from males one day prior to assay setup was done to reduce the number of eggs laid within the activity tubes, as sometimes first instar larvae were seen to have had hatched in the course of the assay. However, even in such cases, the low nutrient food medium prevented further larval growth.

The recordings were done using DAM2 monitors (*Drosophila* Activity Monitoring system, Trikinetics, Waltham, MA, USA). This system works on the beam breaking principle, wherein fly movement past a detector obstructs detection of an infra-red beam, resulting in an activity count. These monitors were lodged in well-humidified incubators (DR-36VLC8 Percival Scientific Inc., Perry, IA, USA), for a maximum of seven days (excluding the day of the setup), under LD 12:12 conditions. As mentioned previously, two light intensities were used across experiments – a high light intensity of 400-500 lux and a low light intensity of 1-1.5 lux. For the first two days of the assay, ambient temperature was maintained at 21 °C, to keep the temperature-sensitive cation channel *dTRPA1* inactive (referred as pre-activation). At ZT 0 on the third day, temperature was increased to and maintained at 29 °C for the following two (or, three) days to hyper-excite the targeted neurons by activating *dTRPA1* (referred to as activation). Following this period of

Dvpdf GAL4 > UAS GFP

A

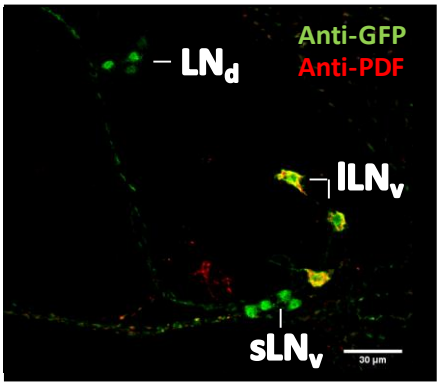

Table 2.2

CELL TYPE	sLN_v (PDF^{+ve})	5th sLN_v (PDF^{-ve})	lLN_v	LN_d
Average	3.1	0.1	3.4	3.3
Range	0 - 4	0 - 1	2 - 4	2 - 5

Mai179 GAL4 > UAS GFP

B

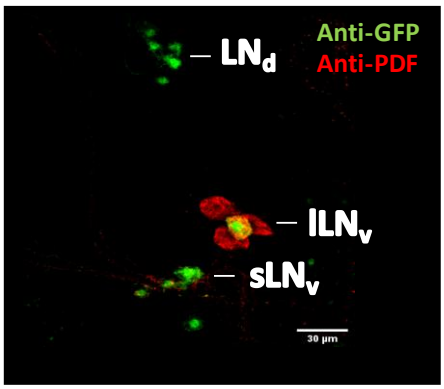

Table 2.3

CELL TYPE	sLN_v (PDF^{+ve})	5th sLN_v (PDF^{-ve})	lLN_v	LN_d
Average	3.1	0.6	1.5	4.4
Range	2 - 4	0 - 1	0 - 4	2 - 6

Mai179 GAL4; Pdf GAL80 > UAS GFP

C

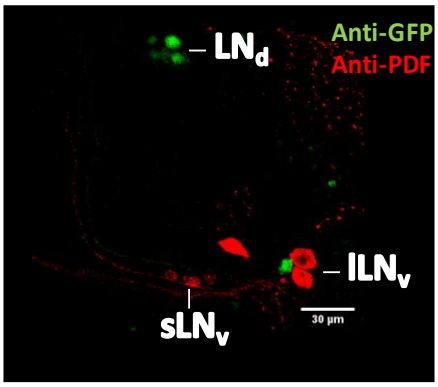

Table 2.4

CELL TYPE	sLN_v (PDF^{+ve})	5th sLN_v (PDF^{-ve})	lLN_v	LN_d
Average	0	0.3	0.2	4
Range	0	0 - 1	0 - 1	2 - 6

Figure 2.2. ***Expression pattern of GAL4 drivers targeting the lateral neuronal cluster*.**
(A) Representative image of *Dvpdf GAL4* expression in s-LN_v and l-LN_v seen from the colocalization of GFP and PDF (Pigment Dispersing Factor – marker for LN_v cells) stains, and in LN_ds identified by GFP. Cell counts (arithmetic mean and range) within each subset are depicted in Table 2.2. (B) Representative image of *Mai179 GAL4* expression among the LN cluster of circadian neurons, with cell counts depicted in Table 2.3. (C) Representative image of *Mai179 GAL4; Pdf GAL80* driver with no GFP expression in PDF^{+ve} LN_v neurons, and cell counts in Table 2.4. *n* = 11-16 brain hemispheres. Scale bars are 30 µm.

activation, temperature was reset and maintained at 21 °C for two more days, to deactivate the channel and restore the neuronal activity (referred as post-activation).

To quantify sleep, activity counts were recorded at 1-minute interval, and scanned using 1-minute bins by the DAMFileScan110 software (Trikinetics, Waltham, MA, USA). Sleep parameters such as daytime and nighttime sleep duration, average bout duration, bout number and activity per waking minute were quantified using PySolo (Gilestro & Cirelli, 2009), while sleep profiles and sleep latency were obtained using a custom-made Microsoft Excel spreadsheet template.

2.2.4 Statistical Analysis – To calculate percentage change in sleep for each fly, change in sleep duration between pre-activation and during/post activation was quantified and normalized against pre-activation sleep of the same time window. Thus, percentage loss in daytime sleep due to *dTRPA1*-mediated heat activation of clock neurons was calculated as (averaged daytime sleep during two days of pre-activation – averaged daytime sleep during two days of activation) / (averaged pre-activation daytime sleep) * 100. Percentage loss in nighttime sleep was similarly calculated by replacing daytime sleep duration with nighttime sleep duration in the above formula. To calculate percentage sleep recovery, sleep duration of varying hours during the first day of post-activation was considered. For example, percentage gain in sleep during 12 hr post-activation was calculated as (daytime sleep of first day post-activation – averaged daytime sleep during two days of pre-activation) / (averaged pre-activation daytime sleep) * 100.

For comparison of percentage change in sleep across genotypes, a one-way ANOVA was conducted, followed by Tukey's Honest Significant Difference (HSD) *post-hoc* test for multiple comparisons. To compare sleep duration, average bout duration, bout number and activity per waking minute across genotypes, repeated measures ANOVA was conducted with genotypes as fixed factor and day/temperature as the repeated measure, followed by Tukey's Honest Significant Difference (HSD) *post-hoc* test. In *post-hoc* comparisons following repeated measures ANOVA, I first looked for differences during pre-activation across genotypes, and second for differences between both days of pre-activation, and activation/post-activation within a genotype. Whenever the assumption of homogeneity of variances was not met (as detected by Levene's test), data was first transformed to equalize variances before conducting ANOVA. All these tests were conducted

using the Statistica 7 software. For comparison of sleep latency (a measure of time spent since lights OFF at ZT 0 till initiation of first sleep bout), Kruskal-Wallis ANOVA by ranks was conducted, followed by Nemenyi *post-hoc* test using R software. Significance level for all tests was set at $p < 0.05$, which has been indicated by horizonal lines and asterisks in the figures. Further details of statistical analyses are mentioned in results and appendices 2.1 and 2.2. All figures were plotted in MS Excel, except for sleep latency for which Sigma Plot (version 11.0) was used.

2.3 Results:

2.3.1 CRY^{-ve} LN$_d$s form part of a wake circuit – I conducted a similar assay as mentioned in Potdar S., *PhD Thesis*, wherein heat-induced activation of subsets of lateral neurons were carried out (by expressing *UAS dTRPA1* via *Dvpdf GAL4* driver). Previously, quantification of sleep showed that the experimental flies slept less compared to controls during activation (Section 2.1). However, it was not known whether this decrease in sleep was significant compared to pre-activation, which would signify true sleep loss. Also, the cause of this sleep loss had not been elucidated. So, I analyzed the results in greater details to further conclude about the function of the targeted cells within the broader sleep circuit. I observed similar levels of baseline sleep among the control (*UAS dTRPA1/+* and *Dvpdf GAL4/+*) and experimental (*Dvpdf GAL4 > UAS dTRPA1*) genotypes, prior to activation (Figure 2.3 A). After the temperature was raised to 29 °C, the experimental flies underwent reduction in sleep, which was more acute on first day of activation (Figure 2.3 A). This could be due to an effect of compensatory (homeostatic) mechanisms trying to make up for the increasing sleep need. The reduction in sleep was quantified as percentage loss of sleep during daytime (lights ON) (Figure 2.3 B) and nighttime (lights OFF) (Figure 2.3 C), and was found to be significantly different from controls in both cases (One-way ANOVA followed by Tukey's *post-hoc* test, $p = 0.0001$ compared to both controls, in both cases). The percentage gain in sleep seen for control flies during daytime (Figure 2.3 B) is due to presence of warmer temperature, a previously observed behavior in wild-type flies (Parisky *et al*., 2016). The sleep loss underwent by the experimental flies led to their higher sleep levels post-activation (Figure 2.3 A, pointed out by an arrow), as was previously described (Potdar S., *PhD Thesis*). To quantify this, I calculated percentage gain in sleep by considering recovery period of 24 h (statistically

significant compared to *UAS* parental control only, $p = 0.004$, data not shown) and 12 h (Figure 2.3 D) (values transformed by cube root to conduct one-way ANOVA followed by Tukey's *post-hoc* test, $p = 0.003$ and $p = 0.007$ compared to *UAS* and *GAL4* parental controls, respectively). Thus, it was concluded that sleep deprivation for 48 h mediated by transient neuronal hyperactivation resulted in sleep rebound for the subsequent 12 h.

To identify the factor causing this sleep change, I next estimated activity index, average sleep bout length and sleep bout number across the six days of assay. For representation however, the baseline sleep parameter plotted (Figure 2.4 A-E) is an average of two days of pre-activation (significant differences compared to both days of baseline have been shown). Also, the second day of recovery has not been shown because no significant effects could be detected when this day was compared to baseline. To determine whether the loss in sleep was resulting from a change in locomotion caused by the temperature rise/activation, activity per waking minute was quantified for all the three genotypes (Figure 2.4 A). Maximal sleep loss for the experimental flies occurred on the first day of activation, however activity counts per waking minute on this day was not statistically different compared to both days of pre-activation (Repeated measures ANOVA followed by Tukey's *post-hoc* test, $p = 0.92$ and $p = 0.67$ when compared to day 1 and 2, respectively). Instead, the experimental flies show reduced activity on second day of activation (Repeated measures ANOVA followed by Tukey's *post-hoc* test, $p = 0.006$ and $p = 0.034$ when compared to day 1 and 2 of baseline, respectively), thus verifying that the reported sleep loss was not a result of increased waking activity. Similarly, sleep gain shown by the experimental flies post-activation, was not caused by a decreased rate of activity (Repeated measures ANOVA followed by Tukey's *post-hoc* test, $p = 0.9$ and $p = 1$ when compared to day 1 and 2 of baseline, respectively). While quantifying the two sleep functions – bout length and number, it was seen that activation decreased daytime average sleep bout length (Figure 2.4 B) on first day of activation in experimental flies (values transformed to power of 0.2 for conducting repeated measures ANOVA followed by Tukey's *post-hoc* test, $p = 0.00003$ on both days of baseline), but second day of activation was only significant compared to day 2 of baseline (Repeated measures ANOVA followed by Tukey's *post-hoc* test, $p = 0.84$ and $p = 0.1$ when compared to day 1 and 2 of baseline, respectively). However at night, bout length (Figure 2.4 C) for both controls and experimental flies significantly decreased, although the experimental genotype showed more sustained and significant reduction (values

transformed to power of 0.2 for conducting repeated measures ANOVA followed by Tukey's *post-hoc* test, $p < 0.0003$ for *UAS dTRPA1* when day 1 of activation was compared to both days of baseline; $p < 0.00009$ and $p < 0.012$ for *Dvpdf GAL4* when day 1 and 2 of activation was compared to both days of baseline, respectively; and $p = 0.00003$ for *Dvpdf GAL4 > UAS dTRPA1*, both days of activation compared to both days of baseline, individually). No such reduction was seen in bout number in response to neuronal hyper-activation during either day or night (Figure 2.4 D & E). Instead, an increase in bout number for the experimental genotype occurred on the second night of activation (Figure 2.4 E) (values transformed by square root to conduct repeated measures ANOVA followed by Tukey's *post-hoc* test, $p = 0.00003$ on both days of baseline), corresponding to the slight increase in sleep seen in Figure 2.3 A, day 4, 84-96 h. The increase in bout number validates the previous suggestion of compensatory mechanisms acting in to cope up for the sustained sleep loss. This interpretation is supported by an increase in bout number for the control flies (Repeated measures ANOVA followed by Tukey's *post-hoc* test, $p < 0.034$ for *UAS dTRPA1* and $p < 0.025$ for *Dvpdf GAL4* when day 1 and 2 of activation was compared to both days of baseline, respectively), as they too undergo sleep loss at night to some extent (Figure 2.3 C & 2.4 C). Moreover, a daytime increase in bout number (Figure 2.4 D) was seen post-activation for experimental flies (values transformed by square root to conduct repeated measures ANOVA followed by Tukey's *post-hoc* test, $p = 0.00004$ and $p = 0.00003$ compared to day 1 and 2 of baseline, respectively), when they were undergoing sleep recovery – a homeostatic response. The decrease in bout length along with an unaffected bout number during activation suggests that hyper-activation of the targeted cells disrupts sleep maintenance, without hampering sleep initiation. On the contrary, the compensatory/homeostatic response is always correlated with an increased bout number, thus suggesting that the core homeostat induces sleep by initiating sleep more frequently. Hence, it was inferred that the targeted evening neurons – majorly consisting of the three CRY^{-ve} LN_ds (Figure 2.2 A & Table 2.2; among the evening neurons targeted by *Dvpdf GAL4* driver – described in Section 2.1, three LN_ds were mostly visible) might be functioning as a wake center, which when activated can trigger a response by the core homeostat.

The representative run shown here was conducted with all fly lines backcrossed prior to two years. Afterwards, for the replicate runs I used an *UAS dTRPA1* line recently backcrossed for an additional two generations. I conducted two independent replicate runs, denoted as replicate

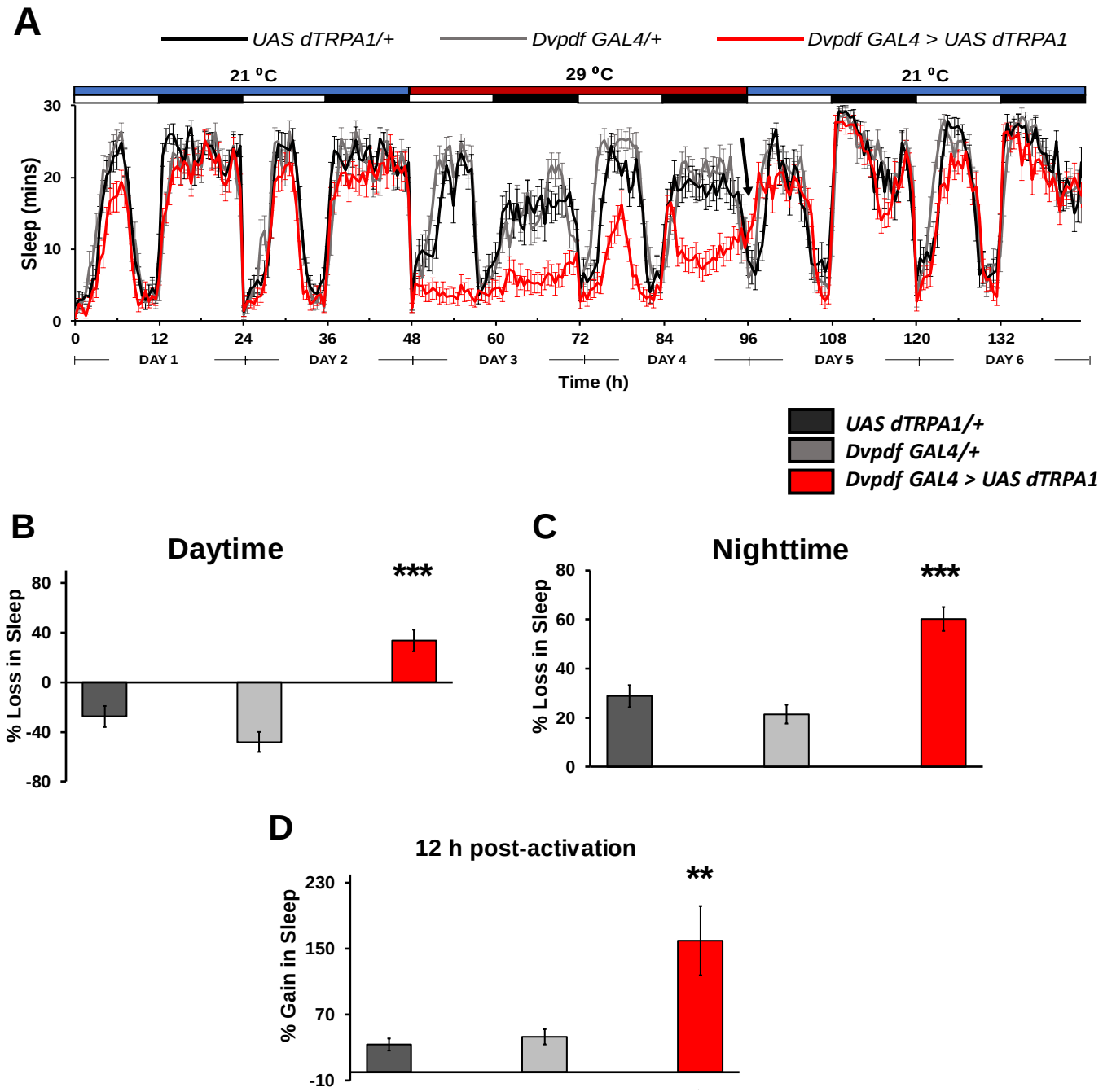

Figure 2.3. ***Changes in sleep architecture due to temperature-mediated hyper-activation of Dvpdf GAL4 flies.*** (A) Sleep per 30 minutes plotted across six days – days 1 and 2 of low temperature (21 °C, blue bar), followed by two days of high temperature (29 °C, dark-red bar), and ending with two days of low temperature. The light regime of LD 12:12 is denoted by white (12 h of light) and black (12 h of dark) bars. Experimental flies lose sleep at 29 °C, which is recovered post-activation (pointed by an arrow). (B-D) Percentage change in sleep at 29 and 21 °C, relative to baseline (average of days 1 and 2). (B) *Dvpdf GAL4* targeted flies lose daytime sleep, while controls gain sleep. (C) At night, all flies lose sleep, but *Dvpdf GAL4 > UAS dTRPA1* undergo significantly higher sleep loss. (D) Experimental flies gain sleep during the first 12 h of post-activation. *n* = 24-29 flies. Error bars denote SEM. **p*<0.05, ***p*<0.01, ****p*<0.001.

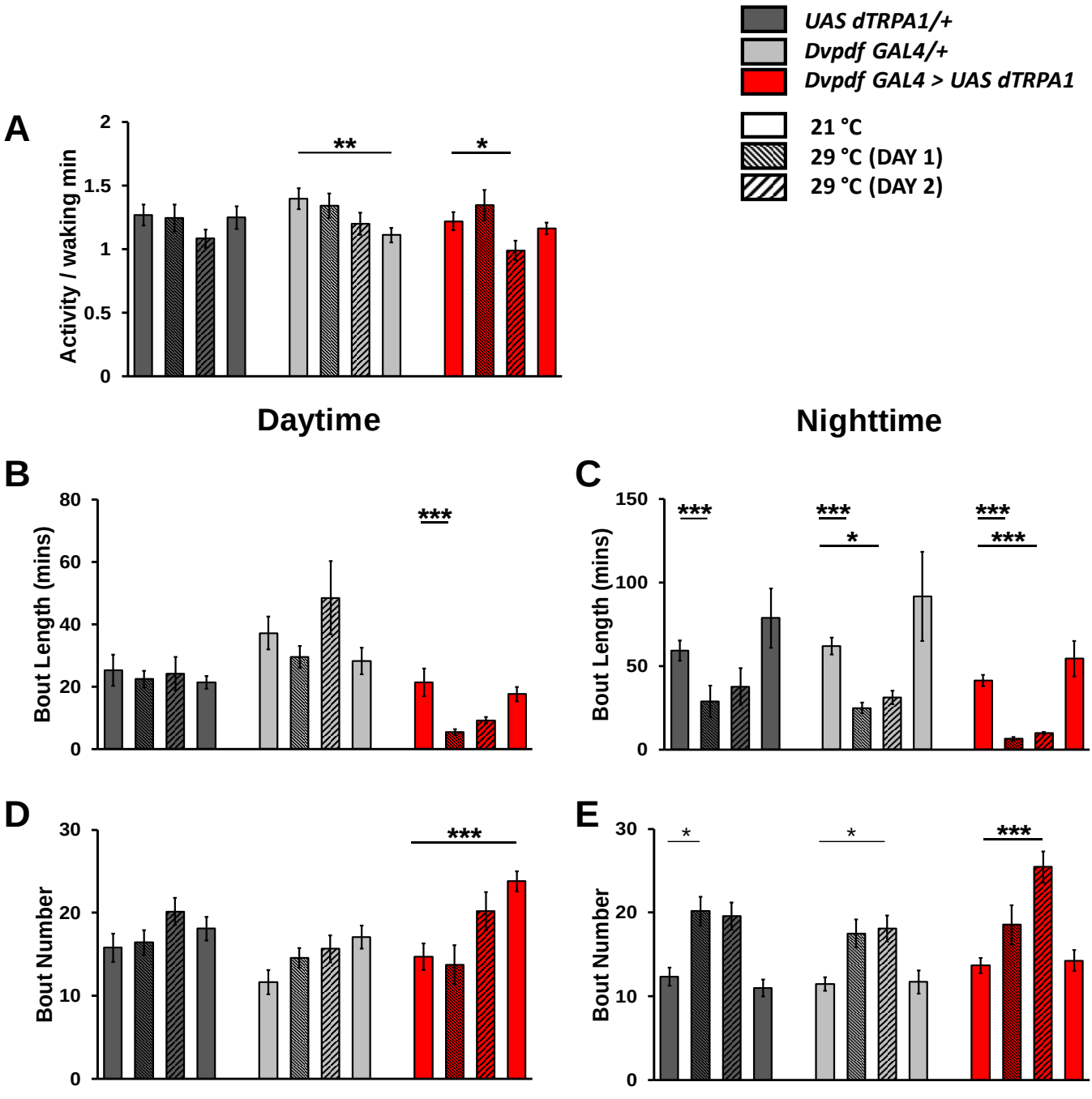

Figure 2.4. ***Effect on activity and sleep structure due to temperature-mediated hyper-activation of Dvpdf GAL4 flies*.** (A) Activity counts per waking minute do not correspond to changes in sleep seen in *Dvpdf GAL4 > UAS dTRPA1*. (B) Daytime and (C) nighttime average sleep bout lengths show most sustained and significant decreases for the experimental genotype at 29 °C, compared to baseline. (D) Increase in number of daytime sleep bouts seen post-activation indicates sleep rebound in experimental flies. (E) Nighttime increase in bout number indicates a homeostatic response to sleep loss caused by high temperature/activation. The first bar for each genotype (at 21 °C) represents the baseline (averaged across two days), while the last bar represents the first day of post-activation. *n* = 24-29 flies. Error bars denote SEM. **p*<0.05, ***p*<0.01, ****p*<0.001.

experiments 1 and 2 (Table 2.5 & 2.6). Replicate experiment 3 (Table 2.7) with an activation period of three days (kept at 29 °C for one more day) was not an independent experiment (had same parents as replicate 1). All parameters of the replicate experiments were analyzed as mentioned above (details regarding transformations for replicate experiments are not shown), the results of which are summarized in Table 2.5-2.7, where the *p*-values refer to the Tukey's *post-hoc* tests (the highest *p*-value has been mentioned wherever *p*-values differed when compared to both parental genotypes). In the replicate runs, slight variations in results were observed, the most notable of which is the reduction in rebound sleep duration. Rebound sleep was calculated for successive durations of 24 h, 12 h, 6 h and 3 h post-activation, with the longest duration showing significant difference from both the parental controls being reported. For an activation period of two days, with recently backcrossed *UAS dTRPA1*, the recovery duration decreased from 12 h to 3 h (Figure 2.3 D & Tables 2.5-2.6). However, the phenomenon of sleep recovery following hyper activation of evening neurons persists, as can be seen from the induction of recovery sleep for 24 h post 3 days of activation (Replicate 3, Table 2.7). In replicate experiment 2, lack of a significant increase in daytime sleep bout number during recovery also complies with the above result – as sleep recovery lasted for a shorter duration, bout number which is calculated for 12 h remained unaffected (Table 2.6). Surprisingly, replicate experiment 3 did not show a change in bout number or length post-activation, corresponding to the 24 h of recovery duration. To conclude, overall results remained similar across replicate runs prior to and post recent backcrossing of *UAS dTRPA1*.

Table 2.5

REPLICATE EXPERIMENT 1	
Daytime sleep loss	Statistically different from both controls ($p = 0.0001$).
Nighttime sleep loss	Statistically different from both controls ($p < 0.02$).
Sleep recovery	Statistically significant for 3 h post-activation ($p = 0.0001$).
Activity index (activity/waking min)	*GAL4/+* and exp. genotypes higher than baseline on day 1 of activation ($p < 0.001$ for *GAL4/+*, $p = 0.00003$ for exp.).
Daytime average sleep bout length	Not significant
Nighttime average sleep bout length	All genotypes lower than BS on both days of activation ($p = 0.00003$ for *UAS/+* and exp., $p < 0.004$ for *GAL4/+*).
Daytime sleep bout number	Controls higher than BS on day 2 of activation ($p < 0.03$). Exp higher than BS during recovery ($p < 0.009$).
Nighttime sleep bout number	All genotypes higher than BS on both days of activation ($p < 0.0001$ – *UAS/+*, $p < 0.006$ – *GAL4/+*, $p < 0.00003$ – exp).

Table 2.5 Replicate experiment 1 of temperature-mediated *Dvpdf GAL4* hyper-activation. The assay was carried out for six days with two days each of baseline, activation and recovery being recorded. To quantify sleep loss and recovery, percentage change in sleep from baseline was calculated (analyzed using One-way ANOVA). For quantifying activity index, bout length and number, all genotypes were compared on baseline days (N.S.), followed by comparisons between activation/recovery with baseline days (analyzed using Repeated measures ANOVA). *UAS dTRPA1* parental flies used for this experiment had been recently backcrossed for two generations. $n = 32$ flies.

Table 2.6

REPLICATE EXPERIMENT 2	
Daytime sleep loss	Statistically different from both controls ($p = 0.0001$).
Nighttime sleep loss	Statistically different only from *GAL4/+* ($p = 0.004$).
Sleep recovery	Statistically significant for 3 h post-activation ($p < 0.03$).
Activity index (activity/waking min)	Only *UAS/+* higher than baseline on day 1 of activation ($p < 0.003$).
Daytime average sleep bout length	*UAS/+* higher from BS during both activation and recovery ($p < 0.006$). Exp. lower than BS on day 1 of activation ($p < 0.001$).
Nighttime average sleep bout length	*UAS/+* higher than BS during recovery ($p < 0.0001$). *GAL4/+* lower than BS on both days of activation ($p < 0.01$). Exp. lower than BS on day 1 of activation ($p < 0.03$).
Daytime sleep bout number	Exp. lower than BS on day 1 of activation ($p < 0.03$).
Nighttime sleep bout number	Both GAL4/+ and exp. higher than BS on both days of activation ($p < 0.00003$ for *GAL4/+*, $p < 0.0001$ for exp.).

Table 2.6 Replicate experiment 2 of temperature-mediated *Dvpdf GAL4* hyper-activation. The assay was carried out for six days with two days each of baseline, activation and recovery being recorded. To quantify sleep loss and recovery, percentage change in sleep from baseline was calculated (analyzed using One-way ANOVA). For quantifying activity index, bout length and number, all genotypes were compared on baseline days (N.S.), followed by comparisons between activation/recovery with baseline days (analyzed using Repeated measures ANOVA). *UAS dTRPA1* parental flies used for this experiment had been recently backcrossed for two generations. n = 29-30 flies.

Table 2.7

REPLICATE EXPERIMENT 3	
Daytime sleep loss	Statistically different from both controls when day 1 of activation is considered ($p < 0.04$).
Nighttime sleep loss	Statistically different from both controls ($p < 0.0001$).
Sleep recovery	Statistically significant for 24 h post-activation ($p < 0.002$).
Activity index (activity/waking min)	*GAL4/+* and exp. genotypes higher than baseline on day 1 of activation ($p < 0.001$ for *GAL4/+*, $p = 0.00004$ for exp.).
Daytime average sleep bout length	*UAS/+* higher than BS on day 3 of activation ($p < 0.002$). *GAL4/+* higher than BS on all days of activation ($p < 0.01$). Exp. lower than BS on day 1 of activation ($p < 0.0001$), and higher on day 3 of activation ($p < 0.01$).
Nighttime average sleep bout length	All genotypes lower than BS on all days of activation (except for *UAS/+* on day 3) ($p = 0.00004$ for *UAS/+* and exp., $p < 0.02$ for *GAL4/+*).
Daytime sleep bout number	Only exp. lower than BS on day 1 of activation ($p = 0.00004$).
Nighttime sleep bout number	*UAS/+* higher than BS on days 1-2 of activation ($p < 0.00004$). *GAL4/+* higher than BS on all days of activation ($p < 0.0002$). Exp. higher than BS on days 2-3 of activation ($p = 0.00004$).

Table 2.7 Replicate experiment 3 of temperature-mediated *Dvpdf GAL4* hyper-activation. The assay was carried out for seven days with two days of baseline, three days of activation and two days of recovery being recorded. To quantify sleep loss and recovery, percentage change in sleep from baseline was calculated (analyzed using One-way ANOVA). For quantifying activity index, bout length and number, all genotypes on baseline days were compared (N.S.), followed by comparisons between activation and recovery with baseline days (analyzed using Repeated measures ANOVA). *UAS dTRPA1* parental flies used for this experiment had been recently backcrossed for two generations. This replicate experiment shared all parental flies with replicate experiment 1. n = 23-30 flies.

2.3.2 CRY^{+ve} LN$_d$s affect sleep dependent on external light condition – It was found previously that hyper-activation of all subsets of the lateral neuronal cluster (both LN$_v$s and LN$_d$s) leads to sleep loss followed by a post-activation recovery, while hyper-activating only the LN$_v$s does not show a similar effect (Section 2.1 & Figure 2.1). Based on the results from this screen, we wanted to exclusively target the LN$_d$s (without involving LN$_v$s) and study the ensuing effect on sleep. The approach previously taken in our lab to do so was to suppress expression from LN$_v$s using *Pdf GAL80* in combination with *Dvpdf GAL4* (by Potdar S.). However, the genotype *Dvpdf GAL4; Pdf GAL80* failed to successfully inhibit GAL4 expression among the LN$_v$s (Potdar S., data not shown), so I used an alternate driver line – *Mai179 GAL4*, which targets similar neuronal subsets as *Dvpdf GAL4* (Figure 2.2 A & B). Using this driver in combination with *Pdf GAL80*, I created a stable line targeting only the LN$_d$s within the LN cluster of circadian clock neurons (Figure 2.2 C). Notwithstanding two brain hemispheres where a single GFP^{+ve} l-LN$_v$ could be detected (Table 2.4), *Mai179 GAL4; Pdf GAL80* can be safely considered as a driver line with very limited/no expression in LN$_v$s. However, the LN$_d$s targeted by this driver are not the same as those targeted by *Dvpdf GAL4* – in this case only the three CRY^{+ve} LN$_d$s are targeted (Rieger *et al*., 2009; Yoshii *et al*., 2008). Therefore, only two cells are common between these two drivers – the 5th s-LN$_v$ and the CRY/ITP co-expressing LN$_d$. My estimates for the number of LN$_d$s targeted by both these drivers are higher than the previous reports, probably because I counted cells irrespective of their staining intensity. At times, I could visualize up to six LN$_d$s per hemisphere (total number of LN$_d$s present), while only 2-3 LN$_d$s would usually be brightly stained.

As earlier, I carried out a similar sleep assay, wherein specific neurons were targeted using heat treatment. I observed that unlike *Dvpdf GAL4*, activation mediated by *Mai179 GAL4 > UAS dTRPA1* did not lead to total sleep deprivation (Figure 2.5 A), even though all LN subsets were targeted here as well. Instead, sleep loss during activation was restricted only to daytime, and nighttime sleep was not prominently affected compared to its parental controls. There are two differences among the neurons targeted by these two drivers – one, *Mai179 GAL4* reportedly targets fewer number of l-LN$_v$s (reported by Shafer & Taghert, 2009; and also seen by me - mentioned in Table 2.3) and second, they target different subsets of LN$_d$s with only one overlapping cell. As mentioned previously (Section 2.1), activation of l-LNvs is known to inhibit sleep at night (Parisky *et al*., 2008; Shang *et al*., 2008; Sheeba *et al*., 2008; and also seen by me -

data not shown). However, if the lack of sleep loss at night was caused due to fewer l-LN_vs being activated by *Mai179* driver, this effect would have been expected to be absent when the LN_vs were exempted from hyper-activation. Yet, *Mai179 GAL4; Pdf GAL80 > UAS dTRPA1* flies were observed to sleep even more at night during activation, as pointed out by arrows (Figure 2.5 A). Therefore, it was hypothesized that the latter difference between both the drivers – that they both target different LN_d subgroups, might be responsible for the difference in sleep pattern during their activation.

To quantify this observed difference in sleep pattern between day and night, I first compared sleep duration (averaged across two days for the first two treatments, and day 1 of post-activation) of *Mai179 GAL4; Pdf GAL80 > UAS dTRPA1* flies (mentioned henceforth as smaller subset) with two of their most relevant parental controls - *Mai179 GAL4; Pdf GAL80/+* and *Mai179 GAL4 > UAS dTRPA1* (mentioned henceforth as larger subset) (Figure 2.5 B & C). At an ambient temperature of 29 °C, wild-type *Drosophila* are known to sleep more during daytime, and lesser at night (Parisky *et al*., 2016). Quantification of sleep duration during activation showed a similar trend for *Mai179 GAL4/+* (Repeated measures ANOVA followed by Tukey's *post-hoc* test, p = 0.00001 for both day and night, compared to respective baseline), but not among the hyper-activated flies. Hyper-exciting both the larger and smaller subsets reduced daytime sleep duration (Repeated measures ANOVA followed by Tukey's *post-hoc* test, p = 0.00001 for both genotypes compared to baseline) (Figure 2.5 B), but a significant nighttime decrease (Figure 2.5 C) in sleep occurred only upon targeting the larger subset (Repeated measures ANOVA followed by Tukey's *post-hoc* test, p = 0.00001 and p = 0.98 compared to baseline for *Mai179 GAL4 > UAS dTRPA1* and *Mai179 GAL4; Pdf GAL80 > UAS dTRPA1*, respectively). This result again highlights that activating a subset of LN_ds along with 5^{th} s-LN_v within the larger LN cluster brings about daytime sleep reduction but does not affect nighttime sleep. To compare the sleep changes observed across genotypes upon activation, I next calculated percentage loss in sleep relative to baseline (Figure 2.6 A & B). To obtain a more complete picture, I also included another genotype *UAS dTRPA1/+*, which is a parental control for *Mai179 GAL4 > UAS dTRPA1*. During daytime (Figure 2.6 A), flies with no artificial neuronal activation showed the expected gain in sleep (as denoted by the negative values when percent loss is plotted), whereas targeting both the larger and smaller subsets induced a sleep loss (one-way ANOVA followed by Tukey's *post-hoc* test, p = 0.00013 compared

to both controls, for both *Mai179 GAL4 > UAS dTRPA1* and *Mai179 GAL4; Pdf GAL80 > UAS dTRPA1*). This suggests that hyper-exciting the LN_ds along with 5^{th} s-LN_v are probably causing daytime sleep loss, and LN_vs do not have any additional effect. Interestingly, at night (Figure 2.6 B) all genotypes lost sleep except for hyper-activated *Mai179 GAL4; Pdf GAL80* (one-way ANOVA followed by Tukey's *post-hoc* test, $p = 0.00013$ compared to all other genotypes). This suggests two possibilities, either the targeted LN_ds are sleep inducing at night, or these flies have a defect in their temperature sensing/processing pathway. I inferred that these LN_ds are sleep inducing, because targeting the larger subset did not alter sleep significantly compared to its controls (*UAS dTRPA1/+* and *Mai179 GAL4; Pdf GAL80/+* – which is close to the GAL4 parental control) even though the LN_vs included in the larger subset promote arousal at night (Parisky *et al*., 2008; Shang *et al*., 2008; Sheeba *et al*., 2008; and also seen by me - data not shown). This is possible only if the LN_ds induced sleep, thus balancing out the inhibitory action of LN_vs.

I next asked whether this induction of daytime loss in sleep resulted in a post-activation sleep recovery. When sleep duration for 24 h post-activation was quantified, similar trends were seen for targeting both the larger and smaller subsets (Figure 2.5 B & C). Both genotypes with artificial neuronal activation showed an increase in daytime sleep duration corresponding to 0-12 h post-activation (Repeated measures ANOVA followed by Tukey's *post-hoc* test for both genotypes, compared to baseline), but a reduction at night corresponding to 12-24 h (Repeated measures ANOVA followed by Tukey's *post-hoc* test, $p = 0.00001$ and $p = 0.005$ compared to baseline, for *Mai179 GAL4 > UAS dTRPA1* and *Mai179 GAL4; Pdf GAL80 > UAS dTRPA1* respectively). Noticeably, post-activation sleep for the non-activated control *Mai179 GAL4; Pdf GAL80/+* did not differ compared to baseline, thus showing that daytime and nighttime changes brought about by higher temperature balanced each other. When this post-activation increase in daytime sleep duration was further quantified to deduce percent gain of sleep (Figure 2.6 C), no significant change was detected (One-way ANOVA, $p = 0.22$). Instead, quantification of percentage change in nighttime sleep (Figure 2.6 D) showed significant sleep losses for both the experimental genotypes, with the severity of sleep loss being higher when the larger subset was targeted (One-way ANOVA followed by Tukey's *post-hoc* test, $p = 0.005$ for *Mai179 GAL4; Pdf GAL80 > UAS dTRPA1* compared to *Mai179 GAL4 > UAS dTRPA1*). This negative sleep rebound for the smaller targeted subset was probably a result of nighttime sleep induction during activation, however no

suitable explanation could be reasoned for the higher sleep loss seen upon targeting the larger subset. One possibility is that the effect of the previous nights' activation continued on even after the temperature was brought down (similar pattern seen for both genotypes in Figures 2.6 B & D).

Another characteristic that seemed to be visibly affected by activation was sleep latency post-lights OFF (Figure 2.5 A). During activation, sleep latency at night decreased remarkably when the smaller subset was targeted (as pointed by the arrows). I quantified this for all the three stages – pre-activation, activation and post-activation (Figure 2.7). During baseline (Figure 2.7 A), latency to fall asleep at night showed no significant difference among all the compared genotypes (Kruskal-Wallis ranked sum test, $p = 0.92$), however the distribution of sleep latency among *Mai179 GAL4; Pdf GAL80 > UAS dTRPA1* flies radically changed during the heat-treatment (Figure 2.7 B) (Kruskal-Wallis ranked sum test followed by Nemenyi *post-hoc* test, $p = 0.00006$ and $p = 0.04$ when compared against *Mai179 GAL4; Pdf GAL80/+* and *Mai179 GAL4 > UAS dTRPA1*, respectively). This result also follows the inference about induction of nighttime sleep on targeting the smaller subset (Figure 2.6 B), because a decrease in sleep latency also signifies a longer sleep duration at night, provided all other sleep parameters (discussed below) remains same. On the first day of post-activation, latency significantly increased for *Mai179 GAL4; Pdf GAL80 > UAS dTRPA1* compared to only one of its parental controls (Kruskal-Wallis ranked sum test followed by Nemenyi *post-hoc* test, $p = 0.0012$ and $p = 0.2$ when compared against *Mai179 GAL4; Pdf GAL80/+* and *Mai179 GAL4 > UAS dTRPA1*, respectively). Thus, it can be concluded that sleep latency prior to and post-activation for *Mai179 GAL4; Pdf GAL80 > UAS dTRPA1* flies was similar to their controls, but it showed a significant reduction during activation.

To test whether these changes in sleep discussed previously all resulted from changes in the behavior of sleep per se, and not from locomotion being affected, activity counts during periods of wakefulness were quantified (Figure 2.8). It was seen that none of the compared genotypes differed amongst each other during baseline (values transformed by power of 0.2 to conduct repeated measures ANOVA followed by Tukey's *post-hoc* test, $p > 0.99$), nor did any genotype differ from its baseline during activation and post-activation (values transformed by power of 0.2 to conduct repeated measures ANOVA followed by Tukey's *post-hoc* test, $p > 0.06$). Thus, it could be concluded that hyper-activation of the targeted neurons affected sleep architecture compared to

baseline, and not fly activity. Thereafter, to explain how neuronal activation affected sleep pattern, I looked for changes in sleep structure – by quantifying bout length and number (Figure 2.8 B-E). However, the only discernible trend that could be identified from these analyses was that daytime sleep loss during activation of *Mai179 GAL4 > UAS dTRPA1* and *Mai179 GAL4; Pdf GAL80 > UAS dTRPA1* occurred via sleep fragmentation as bout length (Figure 2.8 B) decreased (values transformed by power of 0.2 to conduct repeated measures ANOVA followed by Tukey's *post-hoc* test, $p = 0.00001$ for both *Mai179 GAL4 > UAS dTRPA1* and *Mai179 GAL4; Pdf GAL80 > UAS dTRPA1*, compared to their respective baseline) but bout number (Figure 2.8 D) remained unchanged (Repeated measures ANOVA followed by Tukey's *post-hoc* test, $p = 0.9$ and $p = 0.4$ for both *Mai179 GAL4 > UAS dTRPA1* and *Mai179 GAL4; Pdf GAL80 > UAS dTRPA1*, compared to their respective baseline). However, no significant change could be deduced for the rest of the parameters, because the controls changed to similar levels as the experimental.

Overall, activation of the CRY^{+ve} LN_ds in concert with the 5^{th} s-LN_v affect sleep differently during day and night. As these four neurons express the blue-light photoreceptor CRYPTOCHROME (CRY), known to be the primary circadian photoreceptor, it seems likely that these targeted neurons might be controlling sleep in accordance with the presence of light in the external environment. The representative results discussed here were obtained from an assay conducted with all fly lines backcrossed prior to two years. Afterwards, for the replicate runs I used an *UAS dTRPA1* line recently backcrossed for two additional generations by me. I conducted two independent replicate assays under the same experimental conditions, denoted as replicate experiments 1 and 2. All parameters of the replicate experiments were analyzed as mentioned above (details regarding transformations for replicate experiments are not mentioned), and the most important results are summarized in Table 2.8-2.9, where the *p*-values refer to the Tukey's *post-hoc* tests (the highest *p*-value has been mentioned wherever *p*-values differed). In the replicate runs, the general trends discussed above were retained. Thus, it could be concluded that the results prior to and post recent backcrossing of *UAS dTRPA1* remains similar across replicate runs.

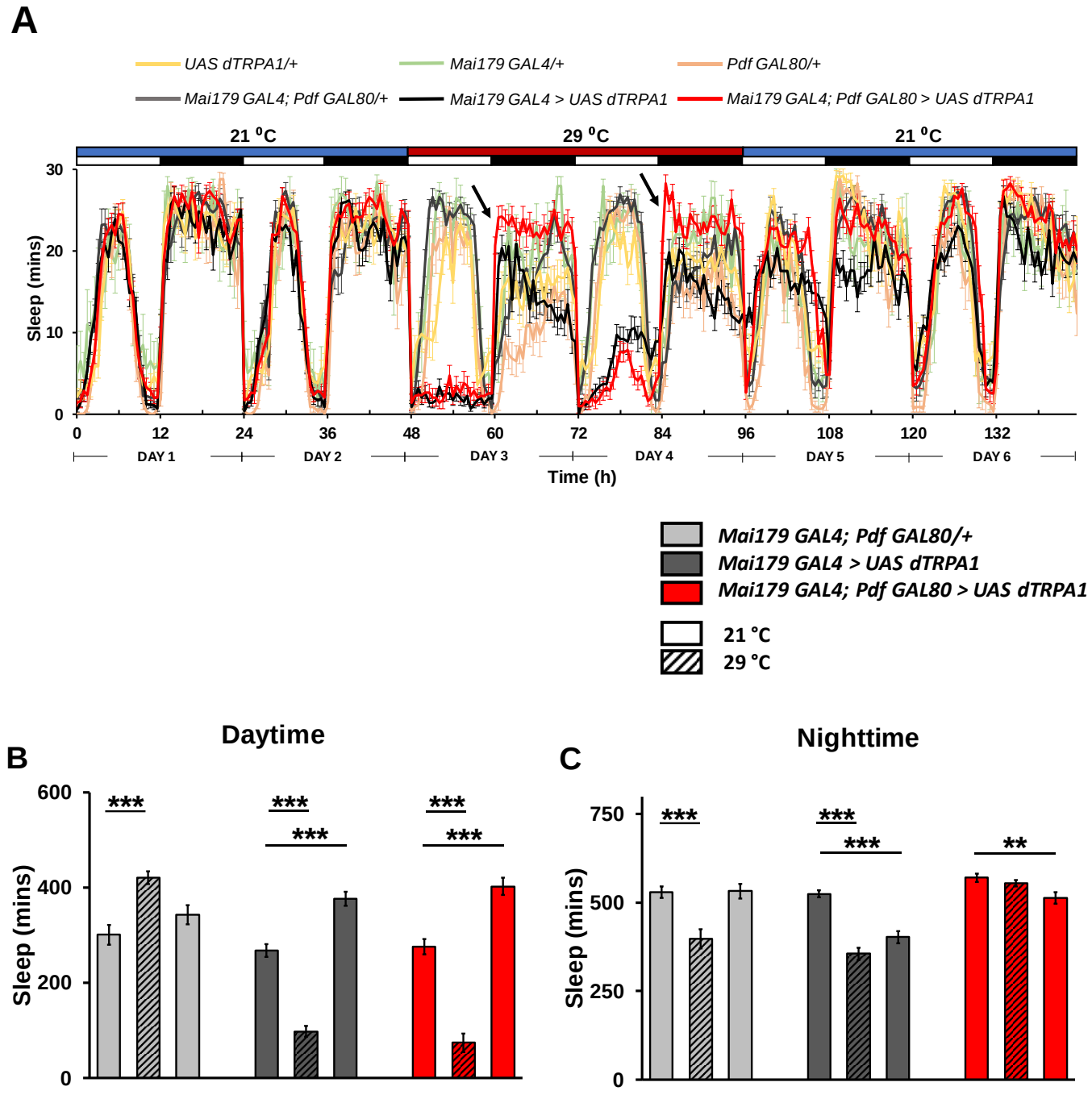

Figure 2.5. ***Sleep architecture and duration upon temperature-mediated hyper-activation of Mai179 GAL4; Pdf GAL80 flies*.** (A) Sleep per 30 minutes plotted across six days – days 1 and 2 of low temperature (21 °C, blue bar), followed by two days of high temperature (29 °C, dark-red bar), and ending with two days of low temperature again. The light regime of LD 12:12 is denoted by white (12 h of light) and black (12 h of dark) bars. Both the experimental genotypes (red and black) lose sleep during day but not at night, during activation. Targeting the smaller subset reduces nighttime sleep latency (pointed by arrows). (B-C) Averaged sleep duration across two days of baseline (first bar) and activation (second bar), followed by first day of recovery. *n* = 30-32 flies. Error bars denote SEM. **p*<0.05, ***p*<0.01, ****p*<0.001.

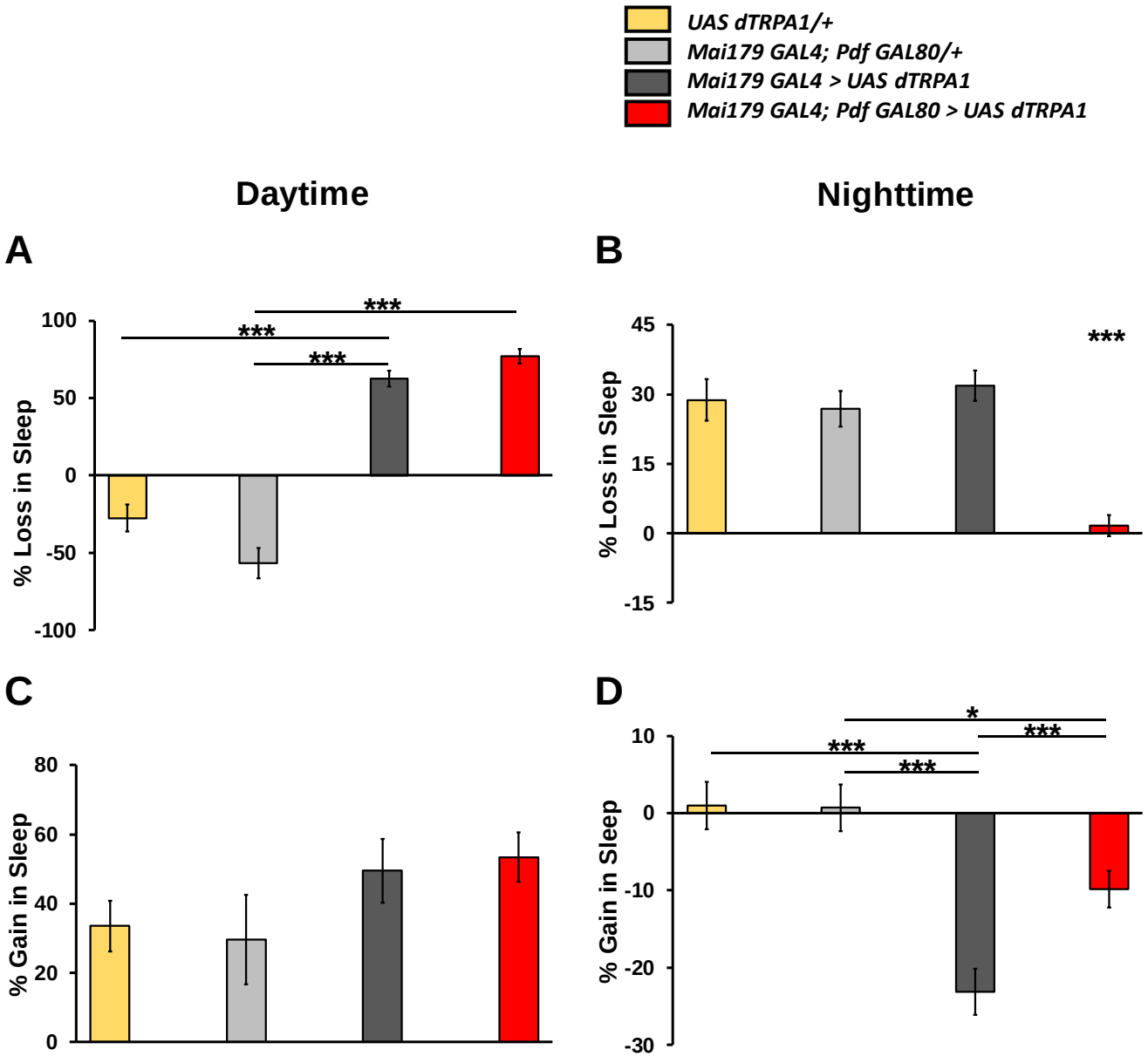

Figure 2.6. ***Characterization of changes in sleep architecture due to temperature-mediated hyper-activation of Mai179 GAL4; Pdf GAL80 flies*.** (A-D) Percentage change in sleep during activation (29 °C) and post-activation (21 °C), relative to baseline. (A) Both *Mai179 GAL4* and *Mai179 GAL4; Pdf GAL80* targeted flies lose daytime sleep upon activation, while non-activated controls gain sleep. (B) At night, all genotypes lose sleep, except for *Mai179 GAL4; Pdf GAL80 > UAS dTRPA1*. (C) No significant sleep recovery is seen between 0-12 h post-activation. (D) On the first night post-activation, both *Mai179 GAL4* and *Mai179 GAL4; Pdf GAL80* targeted flies lose significant amount of sleep compared to the controls. *n* = 30-32 flies. Error bars denote SEM. **p*<0.05, ***p*<0.01, ****p*<0.001.

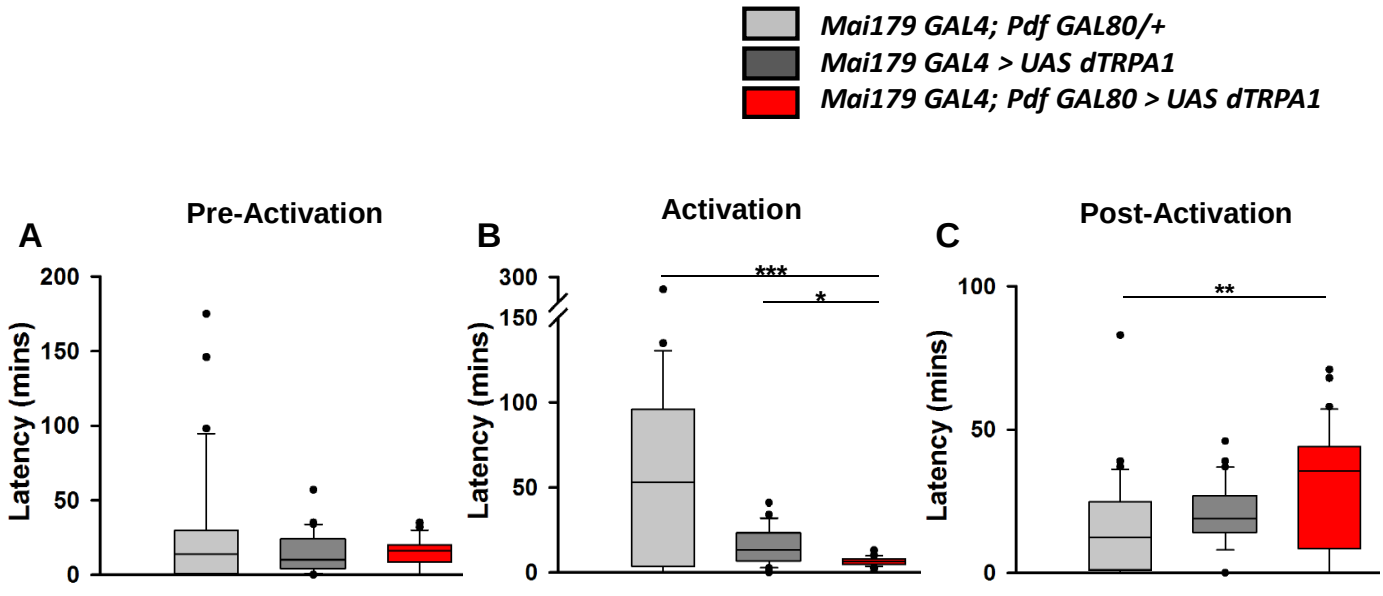

Figure 2.7. ***Changes in sleep latency prior to, during and after temperature-mediated hyper-activation of Mai179 GAL4; Pdf GAL80 flies.*** (A) On the second day of baseline measurements, latency to fall asleep post-lights OFF did not show significant differences across genotypes. (B) During activation, *Mai179 GAL4; Pdf GAL80 > UAS dTRPA1* flies showed significant reduction in sleep latency, compared to both controls (averaged across both days of activation). (C) On the first day of post-activation, latency for *Mai179 GAL4; Pdf GAL80 > UAS dTRPA1* flies showed an increase with respect to only one control. Median sleep latency for all genotypes has been plotted, with the lower and upper edges of the box denoting 25th and 75th percentile, respectively. The lower and upper whiskers denote 10th and 90th percentile, respectively. n = 30-32 flies. *p<0.05, **p<0.01, ***p<0.001.

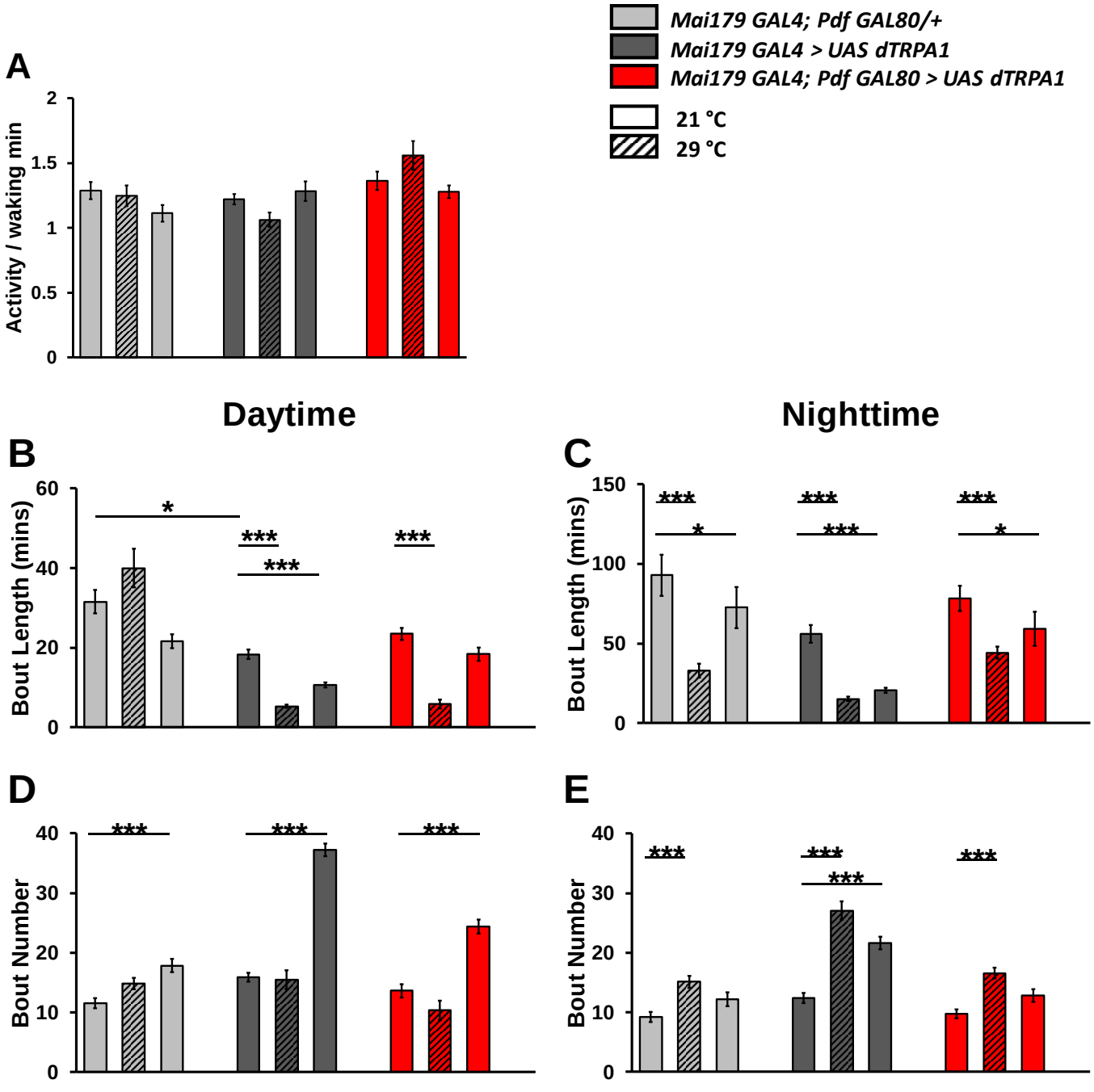

Figure 2.8. ***Effects on activity and sleep structure due to temperature-mediated hyper-activation of Mai179 GAL4; Pdf GAL80 flies*.** (A) Activity counts per waking minute do not show significant changes during baseline, activation and recovery periods. (B) Daytime and (C) nighttime average sleep bout length. For hyper-activated flies, daytime bout length decreases corresponding to sleep loss during activation. All genotypes sustain similar changes for nighttime average bout length. (D) Daytime and (E) nighttime bout number. Again, all genotypes sustain similar trend due to temperature/neuronal activation, with bout numbers increasing at day and decreasing at night. The first two bars for each genotype represent averaged values (across two days) for baseline (at 21 °C) and activation (29 °C), while the last bar represents first day of post-activation. *n* = 30-32 flies. Error bars denote SEM. **p*<0.05, ***p*<0.01, ****p*<0.001.

Table 2.8

REPLICATE EXPERIMENT 1	
Daytime sleep loss	Both *Mai179 GAL4 > UAS dTRPA1* and *Mai179 GAL4; Pdf GAL80 > UAS dTRPA1* significantly higher from the two non-hyperactivated controls ($p < 0.001$).
Nighttime sleep loss	*Mai179 GAL4; Pdf GAL80 > UAS dTRPA1* significantly lower than both non-hyperactivated controls ($p < 0.0009$).
Daytime sleep recovery (0-12 h)	Not significant.
Nighttime sleep recovery (12-24 h)	*Mai179 GAL4 > UAS dTRPA1* significantly lower from only its *UAS* parental control ($p < 0.007$).

Table 2.8 Replicate experiment 1 of temperature-mediated *Mai179 GAL4; Pdf GAL80* hyperactivation. The assay was carried out for six days with two days each of baseline, activation and recovery being recorded. To quantify sleep loss and recovery, % change in sleep from baseline was calculated (One-way ANOVA). *UAS dTRPA1* parental flies used for this experiment had been recently backcrossed for two generations. *n* = 14-32 flies.

Table 2.9

REPLICATE EXPERIMENT 2	
Daytime sleep loss	Both *Mai179 GAL4 > UAS dTRPA1* and *Mai179 GAL4; Pdf GAL80 > UAS dTRPA1* significantly higher from the two non-hyperactivated controls ($p = 0.0001$).
Nighttime sleep loss	*Mai179 GAL4; Pdf GAL80 > UAS dTRPA1* significantly lower from all other genotypes ($p = 0.0001$).
Daytime sleep recovery (0-12 h)	Neither experimental genotype significantly different from both its controls.
Nighttime sleep recovery (12-24 h)	*Mai179 GAL4 > UAS dTRPA1* significantly lower from both its controls ($p = 0.0001$). *Mai179 GAL4; Pdf GAL80 > UAS dTRPA1* significantly lower from *UAS dTRPA1* and *Mai179 GAL4 > UAS dTRPA1* ($p < 0.0003$).

Table 2.9 Replicate experiment 2 of temperature-mediated *Mai179 GAL4; Pdf GAL80* hyperactivation. The assay was carried out for six days with two days each of baseline, activation and recovery being recorded. To quantify sleep loss and recovery, % change in sleep from baseline was calculated (One-way ANOVA). *UAS dTRPA1* parental flies used for this experiment had been recently backcrossed for two generations. *n* = 30-32 flies.

2.3.3 Light affects different subsets of LN_ds differently – In the previous section, I discussed hyper-activating CRY^{+ve} LN_ds might be affecting sleep differently, depending on the external light condition. To test this further, I conducted the same experiment under a very low light intensity (~1 lux). Using the same drivers to target both the subsets of LN_ds – CRY^{-ve} and CRY^{+ve}, I recorded sleep during one day of baseline (at 21 °C), two days of hyper-activation (at 29 °C) and one day of recovery (at 21 °C). From the sleep profiles (Figure 2.9 A & B), it can be seen that hyper-activation of cells targeted by *Dvpdf GAL4* affected sleep similarly both at high and low light intensities. However, flies targeted using *Mai179 GAL4; Pdf GAL80* showed different behavior under different light intensities. At high light intensity, the day-to-night transition (lights ON-OFF) is sharp (Figure 2.5 A), but at low light intensity there is a gradual increase in sleep only for this genotype (Figure 2.9 B, pointed by arrows). This result again favors the hypothesis that LN_d subsets affect sleep varyingly, under different light conditions.

2.4 Discussion:

The stated results suggest differential regulation of sleep by the LN_ds, a subset of circadian pacemaker cells located in the fly brain. To summarize, CRY^{-ve} dorsolateral neurons might function as wake promoting irrespective of external lighting, whereas their CRY^{+ve} counterparts might be regulated by light – sleep-inhibiting in presence of bright light and sleep-inducing in dark (Figure 2.10). However, there are multiple caveats associated with this conclusion. While conducting these assays, activating the CRY^{-ve} LN_ds also included activation of all the LN_v subsets. Similarly, complete restriction of expression within the LN_vs could not be achieved while targeting the CRY^{+ve} LN_ds. Moreover, the 5^{th} s-LN_v (CRY^{+ve}) and the CRY^{+ve}/ITP^{+ve} LN_d were common between both the drivers used. Hence, their role in sleep regulation could not be identified. The driver used for targeting CRY^{+ve} LN_ds (*Mai179 GAL4*) also targets other clock cells (weak expression among few dorsal neurons – Rieger *et al.*, 2009) and non-clock cells (Pars Intercerebralis – Nässel *et al.*, 2008) implicated in sleep regulation (reviewed in Section 1.2). Though these brain regions have not been described for the reported sleep patterns (Section 2.3.2), still an interaction between them and the lateral neuronal cells cannot be ruled out. CRY staining

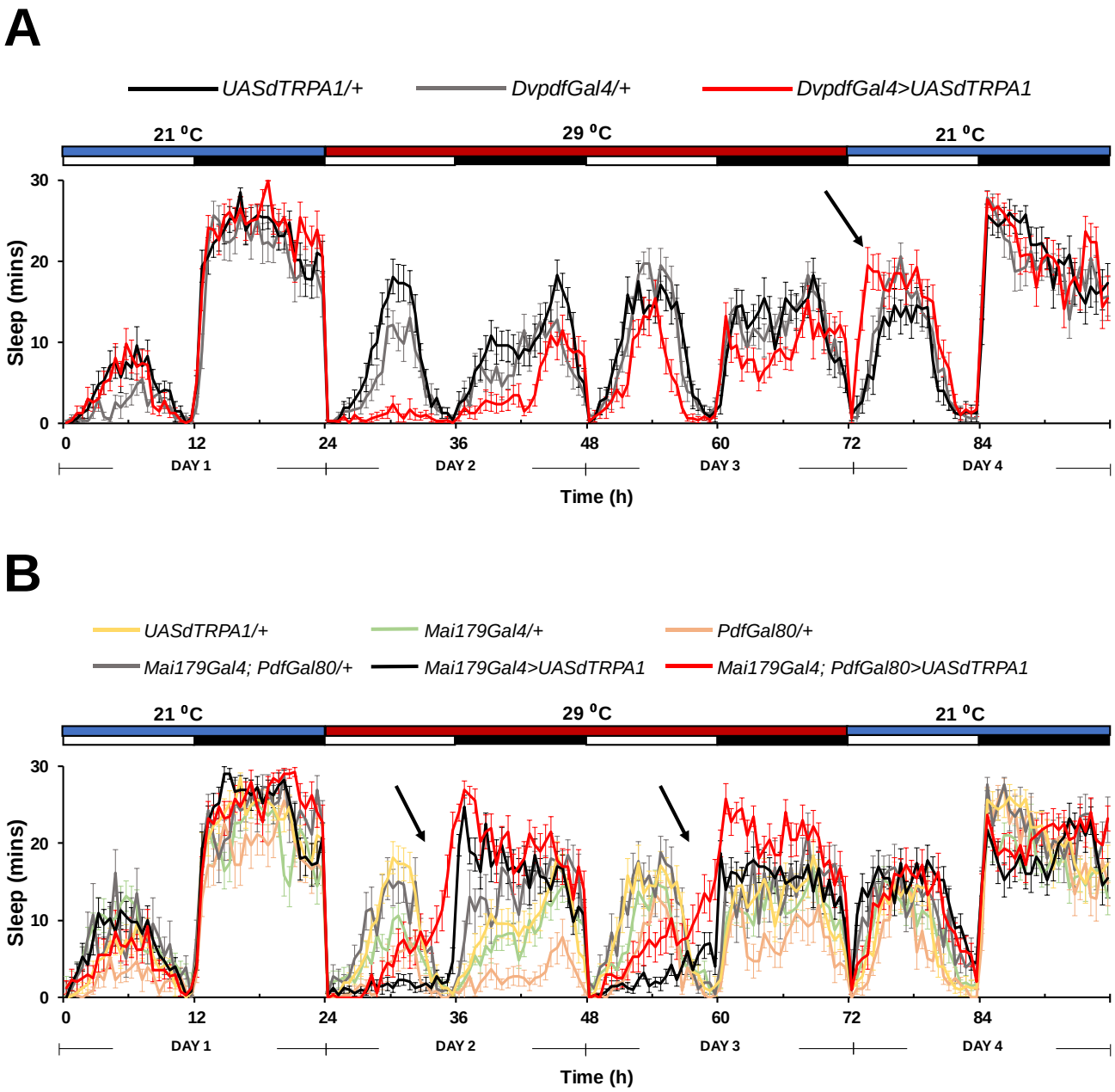

Figure 2.9. ***Sleep pattern upon temperature-mediated hyper-activation of Dvpdf GAL4 and Mai179 GAL4; Pdf GAL80 flies under low-light [1 lux] condition*****.** Sleep per 30 minutes plotted across four days – first day of baseline recording under low temperature (21 °C, blue bar), followed by two days of artificial activation at high temperature (29 °C, dark-red bar), and ending with one day of recovery at low temperature again. The light regime of LD 12:12 is denoted by white (12 h of light) and black (12 h of dark) bars. (A) *Dvpdf GAL4* mediated hyper-activation. The experimental genotype shows sleep loss upon activation, albeit less prominently on the second day. However, this loss is recovered post-activation (pointed by an arrow). (B) *Mai179 GAL4; Pdf GAL80* mediated hyper-activation. These genotypes behave similarly as under high light intensity, except around the lights ON-OFF transition (as pointed by arrows). *n* = 13-32 flies. Error bars denote SEM. Experiment conducted twice with similar results, but data from a single experiment is shown.

could not be carried out successfully due to technical reasons, hence the status of CRY in the targeted neurons was sourced only from literature review.

Keeping in mind these limitations, the conclusive picture that emerges from this study is that of regulation of sleep by the LN_ds. To the best of my knowledge, this is the first study to report the role of all six LN_ds in sleep. Previously, LN_ds had been described as wake-promoting cells (Guo *et al*., 2014; Guo *et al*., 2017 and Guo *et al*., 2018), however none of these studies included the complete set of LN_ds – they mostly targeted the 3-4 *Dvpdf GAL4* expressed LN_ds (Guo *et al*., 2014 and Guo *et al*., 2017). So, the behavior observed upon activating the two CRY^{+ve}/$sNPF^{+ve}$ LN_ds (included in *Mai179 GAL4* driver) is novel. Additionally, the results suggest the presence of sleep-inducing cell(s) within the *Mai179 GAL4* cluster, that are either independent or are inhibited by the PDF^{+ve} cells. Though dorsal neurons fit in this role (both DNs and LN_vs send projections towards each other – Sheeba, 2008 and Guo *et al*., 2018), their effect is more pronounced during midday siesta (Guo *et al*., 2016). Interestingly, daytime sleep is completely abolished in *Mai179 GAL4* targeted flies, thus suggesting involvement of some non-DN cells in the circuit, possibly LN_ds (which also receive input from LN_vs). However, further experiments need to be conducted in order to validate this.

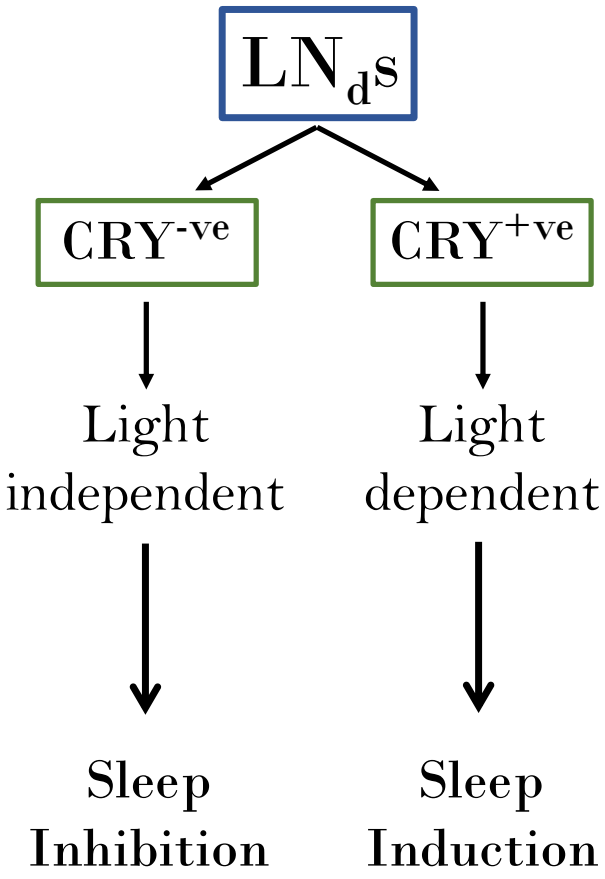

Figure 2.10. ***Functional heterogeneity of LNds in sleep regulation.*** LNds can be broadly divided into two subsets based on the availability of a blue-light photoreceptor CRYPTOCHROME (CRY), implicated in phasing of the molecular clock according to the external light condition. The CRY^{-ve} LNds seem to promote arousal irrespective of availability of light, whereas the CRY^{+ve} LNds might be sleep inhibiting in presence of bright light, and sleep inducing in dark.

CHAPTER 3: CONCLUSION

3.1 LN_ds in non-sleep circuit:

LN_ds were first identified as part of the circadian clock circuit, and have been long known for their function in regulating the evening locomotor bout of activity (Grima *et al*., 2004; Rieger *et al*., 2006; Stoleru *et al*., 2004). It was believed that these evening neurons function subordinate to the master pacemaker (PDF^{+ve} LN_vs, also known as morning neurons), which reset the LN_ds to determine the pace of behavioral rhythms in absence of environmental cues (Stoleru *et al*., 2004). However, more recent findings have dismissed this hierarchical model of circadian pacemaker organization in favour of multiple, independent oscillators being present in the fly brain (Yao & Shafer, 2014 and Bulthuis *et al*., 2019). Yao & Shafer were the first to discover that LN_ds alongwith the 5^{th} s-LN_v can indepedently control activity rhythms even under constant conditions. They also described heterogeneity within the evening neurons and grouped them to three functional classes – two pairs of $PDFR^{+ve}$/$sNPF^{+ve}$/CRY^{+ve} LN_ds to be strongly coupled with PDF^{+ve} neurons, one pair of $PDFR^{+ve}$/ITP^{+ve}/CRY^{+ve} LNd and the 5^{th} s-LN_v to be less strongly coupled and the three pairs of $PDFR^{-ve}$/CRY^{-ve} LN_ds show no direct coupling. Hence, it would not be very surprising if the LN_ds also showed such functional heterogeneity in sleep regulation.

Furthermore, another recent report showed that the evening oscillators can independently affect the neural activity phases of Ellipsoid Body ring neurons . A subset of these ring neurons have been proposed to function as the integrator of sleep homeostat (Liu *et al*., 2016). Therefore, this suggests existance of a communication pathway between the LN_ds and the homeostat, and it might be probable that the LN_ds also transmit sleep information along this pathway.

3.2 Future directions:

The results reported herein asks for several interesting questions to be answered. Firstly, drivers with restricted expression should be used to conduct similar assays. To target CRY^{+ve} LN_ds, drivers such as *R78G02*, *R16C05* and *R54D11* can be used, whereas more than one copy of *Pdf GAL80* can be used in conjugation with *Dvpdf GAL4* to restrict expression to the LN_ds. Even the novel approach reported by Bulthuis *et al*., 2019 to simultaneously target all six LN_ds can provide new insights in sleep regulation by the evening neurons. Deactivating these cells, either electrically or

by blocking chemical transmission, will help to validate the proposed functions of individual LN_d subsets in sleep. It would also be interesting and worthwhile to investigate whether the LN_ds lie downstream to PDF^{+ve} LN_vs in the sleep circuit. In a similar vein, existence of functional pathways can be examined between the LN_ds and the dorsal neurons, as well as the sleep homeostat. This will help to better locate the LN_ds within the sleep circuit. Further experimentation can be conducted to identify the chemical messengers involved in this circuit by using a RNAi based neuropeptide/neurotransmitter screen (using sNPF, NPF, ITP and Cha RNAi).

References

Akerstedt, T., & Gillberg, M. (1981). The circadian variation of experimentally displaced sleep. *Sleep*, *4*(2), 159–169.

Allada, R., & Siegel, J. M. (2008). Unearthing the Phylogenetic Roots of Sleep. *Current Biology*, *18*(15), 14–20.

Artiushin, G., & Sehgal, A. (2017). The Drosophila circuitry of sleep–wake regulation. *Current Opinion in Neurobiology*, 44, 243-253.

Bahn, J. H., Lee, G., & Park, J. H. (2009). Comparative analysis of Pdf-mediated circadian behaviors between Drosophila melanogaster and D. virilis. *Genetics*, *181*(3), 965–975.

Barber, A. F., Erion, R., Holmes, T. C., & Sehgal, A. (2016). Circadian and feeding cues integrate to drive rhythms of physiology in Drosophila insulin-producing cells. *Genes and Development*, *30*(23), 2596–2606.

Beckwith, E. J., & Ceriani, M. F. (2015). Communication between circadian clusters : The key to a plastic network. *FEBS Letters*, *589*(22), 3336–3342.

Borbély, A. A. (1982). A two process model of sleep regulation. *Human Neurobiology*, *1*(3), 195–204.

Borbély, A. A., Daan, S., Wirz-Justice, A., & Deboer, T. (2016). The two-process model of sleep regulation: A reappraisal. *Journal of Sleep Research*, *25*(2), 131–143.

Bulthuis, N., Spontak, K. R., Kleeman, B., & Cavanaugh, D. J. (2019). Neuronal Activity in Non-LNv Clock Cells Is Required to Produce Free-Running Rest:Activity Rhythms in *Drosophila*. *Journal of Biological Rhythms*.

Campbell, S. S., & Tobler, I. (1984). Animal sleep: A review of sleep duration across phylogeny. *Neuroscience and Biobehavioral Reviews*, *8*(3), 269–300.

Cavanaugh, D. J., Geratowski, J. D., Wooltorton, J. R. A., Spaethling, J. M., Hector, C. E., Zheng, X., & Sehgal, A. (2014). Identification of a circadian output circuit for rest: Activity rhythms in drosophila. *Cell*, *157*(3), 689–701.

Chung, B. Y., Kilman, V. L., Keath, J. R., Pitman, J. L., & Allada, R. (2009). The GABAA Receptor RDL Acts in Peptidergic PDF Neurons to Promote Sleep in Drosophila. *Current Biology*, *19*(5), 386–390.

Cirelli, C. (2009). The genetic and molecular regulation of sleep: From fruit flies to humans. *Nature Reviews Neuroscience*, *10*(8), 549–560.

Crocker, A., & Sehgal, A. (2008). Octopamine Regulates Sleep in Drosophila through Protein Kinase A-Dependent Mechanisms. *Journal of Neuroscience*, *28*(38), 9377–9385.

Crocker, A., Shahidullah, M., Levitan, I. B., & Sehgal, A. (2010). Identification of a Neural Circuit that Underlies the Effects of Octopamine on Sleep:Wake Behavior. *Neuron*, *65*(5), 670–681.

Daan, S., Beersma, D. G., & Borbely, A. A. (1984). Timing of human sleep: recovery process gated by a circadian pacemaker. *American Journal of Physiology-Regulatory, Integrative and Comparative Physiology*, *246*(2), 161–183.

Donlea, J. M., Pimentel, D., & Miesenböck, G. (2014). Neuronal machinery of sleep homeostasis in Drosophila. *Neuron*, *81*(4), 860–872.

Donlea, J. M., Pimentel, D., Talbot, C. B., Kempf, A., Omoto, J. J., Hartenstein, V., & Miesenböck, G. (2018). Recurrent Circuitry for Balancing Sleep Need and Sleep. *Neuron*, *97*, 378–389.

Donlea, J. M., Thimgan, M. S., Suzuki, Y., Gottschalk, L., & Shaw, P. J. (2011). Inducing sleep by remote control facilitates memory consolidation in Drosophila. *Science*, *332*(6037), 1571–1576.

Foltenyi, K., Greenspan, R. J., & Newport, J. W. (2007). Activation of EGFR and ERK by rhomboid signaling regulates the consolidation and maintenance of sleep in Drosophila. *Nature Neuroscience*, *10*(9), 1160–1167.

Gilestro, G. F., & Cirelli, C. (2009). PySolo: A complete suite for sleep analysis in Drosophila. *Bioinformatics*, *25*(11), 1466–1467.

Grima, B., Chélot, E., Xia, R., & Rouyer, F. (2004). Morning and evening peaks of activity rely on different clock neurons of the Drosophila brain. *Nature*, *431*(7010), 869–873.

Guo, F., Cerullo, I., Chen, X., & Rosbash, M. (2014). PDF neuron firing phase-shifts key circadian activity neurons in Drosophila. *ELife*, *3*, 1–21.

Guo, F., Chen, X., & Rosbash, M. (2017). Temporal calcium profiling of specific circadian neurons in freely moving flies. *Proceedings of the National Academy of Sciences*, *114*(41), 8780–8787.

Guo, F., Holla, M., Díaz, M. M., & Rosbash, M. (2018). A Circadian Output Circuit Controls Sleep-Wake Arousal in Drosophila. *Neuron*, *100*(3), 624–635.e4.

Guo, F., Yu, J., Jung, H. J., Abruzzi, K. C., Luo, W., Griffith, L. C., & Rosbash, M. (2016). Circadian neuron feedback controls the Drosophila sleep-activity profile. *Nature*, *536*(7616), 292–297.

Hamada, F. N., Rosenzweig, M., Kang, K., Pulver, S. R., Ghezzi, A., Jegla, T. J., & Garrity, P. A. (2008). An internal thermal sensor controlling temperature preference in Drosophila. *Nature*, *454*(7201), 217–220.

Hardin, P. E. (2005). The circadian timekeeping system of Drosophila. *Current Biology*.

Heisenberg, M., Borst, A., Wagner, S., & Byers, D. (1985). *Drosophila* Mushroom Body Mutants are Deficient in Olfactory Learning. *Journal of Neurogenetics*, *2*(1), 1–30.

Hendricks, J. C., Finn, S. M., Panckeri, K. A., Chavkin, J., Williams, J. A., Sehgal, A., & Pack, A. I. (2000). Rest in Drosophila Is a Sleep-like State. *Neuron*, *25*(1), 129–138.

Huber, R., Hill, S. L., Holladay, C., Biesiadecki, M., Tononi, G., & Cirelli, C. (2004). Sleep homeostasis in Drosophila melanogaster. *Sleep*, *27*(4), 628–639.

Jaramillo, A. M., Zheng, X., Zhou, Y., Amado, D. A., Sheldon, A., Sehgal, A., & Levitan, I. B. (2004). Pattern of distribution and cycling of SLOB, Slowpoke channel binding protein, in Drosophila. *BMC Neuroscience*, *5*, 3.

Joiner, W. J., Crocker, A., White, B. H., & Sehgal, A. (2006). Sleep in Drosophila is regulated by adult mushroom bodies. *Nature*, *441*(7094), 757–760.

Koh, K., Evans, J. M., Hendricks, J. C., & Sehgal, A. (2006). A Drosophila model for age-associated changes in sleep:wake cycles. *Proceedings of the National Academy of Sciences*, *103*(37), 13843–13847.

Kunst, M., Hughes, M. E., Raccuglia, D., Felix, M., Li, M., Barnett, G., & Nitabach, M. N. (2014). Calcitonin gene-related peptide neurons mediate sleep-specific circadian output in Drosophila. *Current Biology*, *24*(22), 2652–2664.

Lamaze, A., Krätschmer, P., Chen, K. F., Lowe, S., & Jepson, J. E. C. (2018). A Wake-Promoting Circadian Output Circuit in Drosophila. *Current Biology*, *28*(19), 3098–3105.e3.

Liu, S., Lamaze, A., Liu, Q., Tabuchi, M., Yang, Y., Fowler, M., & Wu, M. N. (2014). WIDE AWAKE mediates the circadian timing of sleep onset. *Neuron*, *82*(1), 151–166.

Liu, S., Liu, Q., Tabuchi, M., & Wu, M. N. (2016). Sleep drive is encoded by neural plastic changes in a dedicated circuit. *Cell*, *165*(6), 1347–1360.

Martin, J.-R., Ernst, R., & Heisenberg, M. (1998). Mushroom bodies suppress locomotor activity in Drosophila melanogaster. *Learning & Memory (Cold Spring Harbor, N.Y.)*, *5*(1–2), 179–191.

McCarley, R. W. (2007). Neurobiology of REM and NREM sleep. *Sleep Medicine*, *8*(4), 302–330.

Nässel, D. R., Enell, L. E., Santos, J. G., Wegener, C., & Johard, H. A. D. (2008). A large population of diverse neurons in the Drosophila central nervous system expresses short neuropeptide F, suggesting multiple distributed peptide functions. *BMC Neuroscience*, *9(1)* 90.

Nitabach, M. N., & Taghert, P. H. (2008). Organization of the Drosophila Circadian Control Circuit. *Current Biology*, *18*(2), 84–93.

Nitz, D. A., Van Swinderen, B., Tononi, G., & Greenspan, R. J. (2002). Electrophysiological correlates of rest and activity in Drosophila melanogaster. *Current Biology*, *12*(22), 1934–1940.

Pan, Y., Zhou, Y., Guo, C., Gong, H., Gong, Z., & Liu, L. (2009). Differential roles of the fan-shaped body and the ellipsoid body in Drosophila visual pattern memory. *Learning and Memory*, *16*(5), 289–295.

Parisky, K. M., Agosto, J., Pulver, S. R., Shang, Y., Kuklin, E., Hodge, J. J. L., & Griffith, L. C. (2008). PDF Cells Are a GABA-Responsive Wake-Promoting Component of the Drosophila Sleep Circuit. *Neuron*, *60*(4), 672–682.

Parisky, K. M., Agosto Rivera, J. L., Donelson, N. C., Kotecha, S., & Griffith, L. C. (2016). Reorganization of Sleep by Temperature in Drosophila Requires Light, the Homeostat, and the Circadian Clock. *Current Biology*, *26*(7), 882–892.

Pimentel, D., Donlea, J. M., Talbot, C. B., Song, S. M., Thurston, A. J. F., & Miesenböck, G. (2016). Operation of a homeostatic sleep switch. *Nature*, *536*(7616), 333–337.

Pitman, J. L., McGill, J. J., Keegan, K. P., & Allada, R. (2006). A dynamic role for the mushroom bodies in promoting sleep in Drosophila. *Nature*, *441*(7094), 753–756.

Potdar, S., & Sheeba, V. (2018). Wakefulness Is Promoted during Day Time by PDFR Signalling to Dopaminergic Neurons in Drosophila melanogaster. *Eneuro*, *5*(4), 1-17.

Rieger, D., Shafer, O. T., Tomioka, K., & Helfrich-fo, C. (2006). Functional Analysis of Circadian Pacemaker Neurons in Drosophila melanogaster (1976) model and suggests that a subgroup of the ventral subset of the small LN acts as " main " oscillator controlling M and E activity bouts, *26*(9), 2531–2543.

Rieger, D., Wülbeck, C., Rouyer, F., & Helfrich-Förster, C. (2009). Period gene expression in four neurons is sufficient for rhythmic activity of drosophila melanogaster under dim light conditions. *Journal of Biological Rhythms*, *24*(4), 271–282.

Rosato, E., Tauber, E., & Kyriacou, C. P. (2006). Molecular genetics of the fruit-fly circadian clock. *European Journal of Human Genetics*, 14, 729-738.

Schubert, F. K., Hagedorn, N., Yoshii, T., Helfrich-Förster, C., & Rieger, D. (2018). Neuroanatomical details of the lateral neurons of Drosophila melanogaster support their functional role in the circadian system. *J. Comparative Neurology*, *526*(7), 1209–1231.

Shafer, O. T., & Taghert, P. H. (2009). RNA-interference knockdown of drosophila pigment dispersing factor in neuronal subsets: The anatomical basis of a neuropeptide's circadian functions. *PLoS ONE*, *4*(12).

Shang, Y., Donelson, N. C., Vecsey, C. G., Guo, F., Rosbash, M., & Griffith, L. C. (2013). Short Neuropeptide F Is a Sleep-Promoting Inhibitory Modulator. *Neuron*, *80*(1), 171–183.

Shang, Y., Griffith, L. C., & Rosbash, M. (2008). Light-arousal and circadian photoreception circuits intersect at the large PDF cells of the Drosophila brain. *Proceedings of the National Academy of Sciences*, *105*(50), 19587–19594.

Shaw, P. J. (2000). Correlates of Sleep and Waking in Drosophila melanogaster. *Science*, *287*(5459), 1834–1837.

Sheeba, V. (2008). The Drosophila melanogaster circadian pacemaker circuit. *Journal of Genetics*, 87(5), 485-493.

Sheeba, V., Fogle, K. J., Kaneko, M., Rashid, S., Chou, Y., Sharma, V. K., & Holmes, T. C. (2008). Large Ventral Lateral Neurons Modulate Arousal and Sleep in Drosophila. *Current Biology*, *18*(20), 1537–1545.

Siegmund, T., & Korge, G. (2001). Innervation of the ring gland of drosophila melanogaster. *Journal of Comparative Neurology*, *431*(4), 481–491.

Sitaraman, D., Aso, Y., Jin, X., Chen, N., Felix, M., Rubin, G. M., & Nitabach, M. N. (2015). Propagation of Homeostatic Sleep Signals by Segregated Synaptic Microcircuits of the Drosophila Mushroom Body. *Current Biology*, *25*(22), 2915–2927.

Stoleru, D., Peng, Y., Agosto, J., & Rosbash, M. (2004). Coupled oscillators control morning and evening locomotor behaviour of Drosophila. *Nature*, *431*(7010), 862–868.

Tabuchi, M., Monaco, J. D., Duan, G., Bell, B., Liu, S., Liu, Q., & Wu, M. N. (2018). Clock-Generated Temporal Codes Determine Synaptic Plasticity to Control Sleep. *Cell*, *175*(5), 1213–1227.

van Alphen, B., Yap, M. H. W., Kirszenblat, L., Kottler, B., & van Swinderen, B. (2013). A Dynamic Deep Sleep Stage in Drosophila. *Journal of Neuroscience*, *33*(16), 6917–6927.

Vienne, J., Spann, R., Guo, F., & Rosbash, M. (2016). Age-Related Reduction of Recovery Sleep and Arousal Threshold in Drosophila. *Sleep*, *39*(8), 1613–1624.

Yadlapalli, S., Jiang, C., Bahle, A., Reddy, P., Meyhofer, E., & Shafer, O. T. (2018). Circadian clock neurons constantly monitor environmental temperature to set sleep timing. *Nature*, *555*(7694), 98–102.

Yao, Z., & Shafer, O. T. (2014). The Drosophila circadian clock is a variably coupled network of multiple peptidergic units. *Science*, *343*(6178), 1516–1520.

Yoshii, T., Todo, T., Wülbeck, C., Stanewsky, R., & Helfrich-Förster, C. (2008). Cryptochrome is present in the compound eyes and a subset of Drosophila's clock neurons. *Journal of Comparative Neurology*, *508*(6), 952–966.

Zheng, X., & Sehgal, A. (2008). Probing the relative importance of molecular oscillations in the circadian clock. *Genetics*, 178(3), 1147-1155.

Appendices

Appendix 1

Fly strain	Source
w^{1118}	BDSC #5905
Dvpdf GAL4	Michael Rosbash
Mai179 GAL4	Todd Holmes
Pdf GAL80	Charlotte Helfrich-Förster
Pdf GAL4	Todd Holmes
UAS dTRPA1	BDSC #26263, NCBS

Appendix 1. Fly strains used along with their respective sources. BDSC – Bloomington Drosophila Stock Centre, Bloomington, IN, USA; NCBS – National Centre for Biological Sciences, Bangalore, India. Other sources - Michael Rosbash (Brandeis University, Waltham, MA, USA), Todd Holmes (University of California, Irvine, CA, USA), Charlotte Helfrich-Förster (Universität Würzberg, Würzberg, Germany).

Appendix 2.1

Appendix 2.1 A

Effect	**df**	**MS**	**F**	***p***
Genotype	2	49314.2	25.8	0.0000

Appendix 2.1 A. One-way ANOVA to compare daytime sleep loss of *Dvpdf GAL4 > UAS dTRPA1* flies during activation.

Appendix 2.1 B

Effect	**df**	**MS**	**F**	***p***
Genotype	2	11532.2	22.1	0.0000

Appendix 2.1 B. One-way ANOVA to compare nighttime sleep loss of *Dvpdf GAL4 > UAS dTRPA1* flies during activation.

Appendix 2.1 C

Effect	**df**	**MS**	**F**	***p***
Genotype	2	39.0	7.2	0.0012

Appendix 2.1 C. One-way ANOVA to compare sleep recovery (12 h) of *Dvpdf GAL4 > UAS dTRPA1* flies post activation. Values were transformed by cube root to satisfy heterogeneity of variances.

Appendix 2.1 D

Effect	**df**	**MS**	**F**	***p***
Genotype	2	0.3	0.4	0.6513
Day	5	0.6	12.2	0.0000
Genotype*Day	10	0.1	2.3	0.0106

Appendix 2.1 D. Repeated measures ANOVA on activity counts per waking minute of *Dvpdf GAL4 > UAS dTRPA1* flies and controls.

Appendix 2.1 E

Effect	df	MS	F	*p*
Genotype	2	5.9	30.9	0.0000
Day	5	1.0	14.5	0.0000
Genotype*Day	10	0.6	9.6	0.0000

Appendix 2.1 E. Repeated measures ANOVA on daytime average sleep bout length of *Dvpdf GAL4 > UAS dTRPA1* flies and controls. Values were transformed to power of 0.2 to satisfy heterogeneity of variances.

Appendix 2.1 F

Effect	df	MS	F	*p*
Genotype	2	2.9	12.9	0.0000
Day	5	4.1	65.8	0.0000
Genotype*Day	10	0.1	2.9	0.0016

Appendix 2.1 F. Repeated measures ANOVA on nighttime average sleep bout length of *Dvpdf GAL4 > UAS dTRPA1* flies and controls. Values were transformed to power of 0.2 to satisfy heterogeneity of variances.

Appendix 2.1 G

Effect	df	MS	F	*p*
Genotype	2	7.6	1.3	0.2608
Day	5	9.2	15.0	0.0000
Genotype*Day	10	2.7	4.5	0.0000

Appendix 2.1 G. Repeated measures ANOVA on daytime sleep bout number of *Dvpdf GAL4 > UAS dTRPA1* flies and controls. Values were transformed to power of 0.5 to satisfy heterogeneity of variances.

Appendix 2.1 H

Effect	df	MS	F	*p*
Genotype	2	6.4	2.5	0.0815
Day	5	16.2	23.0	0.0000
Genotype*Day	10	1.0	1.5	0.1267

Appendix 2.1 H. Repeated measures ANOVA on nighttime sleep bout number of *Dvpdf GAL4 > UAS dTRPA1* flies and controls. Values were transformed to power of 0.5 to satisfy heterogeneity of variances.

Appendix 2.2

Appendix 2.2 A

Effect	df	MS	F	*p*
Genotype	2	354512	18.7	0.0000
Treatment	2	730111	179.7	0.0000
Genotype*Treatment	4	435875	107.3	0.0000

Appendix 2.2 A. Repeated measures ANOVA on daytime sleep duration of *Mai179 GAL4; Pdf GAL80 > UAS dTRPA1* flies and controls.

Appendix 2.2 B

Effect	df	MS	F	*p*
Genotype	2	326326	16.7	0.0000
Treatment	2	262343	72.1	0.0000
Genotype*Treatment	4	95282	26.1	0.0000

Appendix 2.2 B. Repeated measures ANOVA on nighttime sleep duration of *Mai179 GAL4; Pdf GAL80 > UAS dTRPA1* flies and controls.

Appendix 2.2 C

Effect	df	MS	F	*p*
Genotype	3	132818.2	85.0	0.0000

Appendix 2.2 C. One-way ANOVA to compare daytime sleep loss of *Mai179 GAL4; Pdf GAL80 > UAS dTRPA1* flies during activation.

Appendix 2.2 D

Effect	df	MS	F	*p*
Genotype	3	5991.9	17.0	0.0000

Appendix 2.2 D. One-way ANOVA to compare nighttime sleep loss of *Mai179 GAL4; Pdf GAL80 > UAS dTRPA1* flies during activation.

Appendix 2.2 E

Effect	df	MS	F	*p*
Genotype	3	4171.9	1.4	0.2210

Appendix 2.2 E. One-way ANOVA to compare daytime sleep gain (0-12 h) of *Mai179 GAL4; Pdf GAL80 > UAS dTRPA1* flies post activation.

Appendix 2.2 F

Effect	df	MS	F	*p*
Genotype	3	3774.8	15.6	0.0000

Appendix 2.2 F. One-way ANOVA to compare nighttime sleep gain (12-24 h) of *Mai179 GAL4; Pdf GAL80 > UAS dTRPA1* flies post activation.

Appendix 2.2 G

Effect	df	Chi-square	*p*
Genotype	2	0.15	0.9246

Appendix 2.2 G. Kruskal Wallis ranked ANOVA to compare nighttime sleep latency of *Mai179 GAL4; Pdf GAL80 > UAS dTRPA1* flies prior to activation.

Appendix 2.2 H

Effect	df	Chi-square	*p*
Genotype	2	18.12	0.0001

Appendix 2.2 H. Kruskal Wallis ranked ANOVA to compare nighttime sleep latency of *Mai179 GAL4; Pdf GAL80 > UAS dTRPA1* flies during activation.

Appendix 2.2 I

Effect	df	Chi-square	*p*
Genotype	2	12.40	0.0020

Appendix 2.2 H. Kruskal Wallis ranked ANOVA to compare nighttime sleep latency of *Mai179 GAL4; Pdf GAL80 > UAS dTRPA1* flies post activation.

Appendix 2.2 J

Effect	df	MS	F	*p*
Genotype	2	0.02	2.6	0.0797
Treatment	2	0.002	1.7	0.1863
Genotype*Treatment	4	0.01	7.5	0.0000

Appendix 2.2 J. Repeated measures ANOVA on activity counts per waking minute of *Mai179 GAL4; Pdf GAL80 > UAS dTRPA1* flies and controls. Values were transformed to power of 0.2 to satisfy heterogeneity of variances.

Appendix 2.2 K

Effect	df	MS	F	*p*
Genotype	2	3.3	83.1	0.0000
Treatment	2	1.8	54.9	0.0000
Genotype*Treatment	4	1.1	33.1	0.0000

Appendix 2.2 K. Repeated measures ANOVA on daytime average sleep bout length of *Mai179 GAL4; Pdf GAL80 > UAS dTRPA1* flies and controls. Values were transformed to power of 0.2 to satisfy heterogeneity of variances.

Appendix 2.2 L

Effect	df	MS	F	*p*
Genotype	2	2.6	21.8	0.0000
Treatment	2	3.6	88.9	0.0000
Genotype*Treatment	4	0.2	5.7	0.0002

Appendix 2.2 L. Repeated measures ANOVA on nighttime average sleep bout length of *Mai179 GAL4; Pdf GAL80 > UAS dTRPA1* flies and controls. Values were transformed to power of 0.2 to satisfy heterogeneity of variances.

Appendix 2.2 M

Effect	**df**	**MS**	**F**	***p***
Genotype	2	1749.2	30.3	0.0000
Treatment	2	5194.4	144.6	0.0000
Genotype*Treatment	4	820.8	22.8	0.0000

Appendix 2.2 M. Repeated measures ANOVA on daytime sleep bout number of *Mai179 GAL4; Pdf GAL80 > UAS dTRPA1* flies and controls.

Appendix 2.2 N

Effect	**df**	**MS**	**F**	***p***
Genotype	2	168.6	34.7	0.0000
Treatment	2	186.8	77.1	0.0000
Genotype*Treatment	4	13.8	5.7	0.0002

Appendix 2.2 N. Repeated measures ANOVA on nighttime sleep bout number of *Mai179 GAL4; Pdf GAL80 > UAS dTRPA1* flies and controls. Values were transformed to power of 0.7 to satisfy heterogeneity of variances.